USE OF COMPOSITE MATERIALS TO REPAIR STEEL STRUCTURES VULNERABLE TO FATIGUE DAMAGE

By

Fatih Alemdar

Submitted to the graduate degree program in Civil Engineering and the Faculty of the Graduate School of the University of Kansas in partial fulfillment of the requirements for the degree of Master's of Science

Committee:

_____

Chairperson: Dr. Adolfo B. Matamoros

_____

Dr. Caroline Bennett

_____

Dr. Stanley Rolfe

_____

Dr. Ronald Gonzalez Barrett

Date defended: 11/02/2010

The Thesis Committee for Fatih Alemdar certifies

that this is the approved version of the following thesis:

USE OF COMPOSITE MATERIALS TO REPAIR STEEL STRUCTURES VULNERABLE TO FATIGUE DAMAGE

Chairperson Dr. Adolfo B. Matamoros

Date approved: 11/12/2010

ACKNOWLEDGEMENTS

Completion of this project would not have been possible without contributions from the following people:

First, I would like to thank the Kansas Department of Transportation (KDOT) and the University of Kansas Transportation Research Institute (KU TRI). I would like to thank through Pooled Fund Study TPF-5(189), which includes the following participating State DOTs: Kansas, California, Iowa, Illinois, New Jersey, New York, Oregon, Pennsylvania, Tennessee Wisconsin, and Wyoming, as well as the Federal Highway Administration.

I would like to thank the Associated Industries Inc. and Spray Equipment Inc. that donated materials, labor, and other resources to the project.

I would like to thank Drs. Adolfo Matamoros, Caroline Bennett, Ronald M. Barrett-Gonzalez, and Stanley Rolfe for their guidance, expertise, and willingness to help solve issues as they arose during the project. I would like to thank Jim Weaver for providing solutions to the multitude of complications that this project posed. Thanks also to a number of graduate students who helped me lift specimens into and out of the testing machine for the past year.

Lastly, I would like to thank my wife Dr. Zeynep Firat Alemdar for her unending support and encouragement throughout the duration of this project.

TABLE OF CONTENTS

LIST OF FIGURES

LIST OF TABLES

INTRODUCTION

A study was conducted to investigate the use of Carbon Fiber Reinforced Polymers (CFRP's) to prevent and repair fatigue damage to bridge structures, which is a very common problem afflicting older steel bridges with welded connections.

The presence of fatigue cracks in older steel bridges depends on factors such as the frequency of loading and the intensity of loading. For example, the intensity of loading (defined in terms of the stress range) is inversely proportional to the rule of the fatigue life of the structure, with a relationship that is linear when plotted using a logarithmic scale. Another important factor affecting fatigue life is the geometry. For example, regions of a structure that have abrupt changes in geometry connection are most sensitive to fatigue damage.

This study investigates mainly two different topics related to the use of CFRP's for strengthening and repair of steel bridges: the use of CFRP's to prevent damage in fatigue vulnerable welded connections prior to fatigue-crack initiation, and the use of CFRP's to stall the propagation of fatigue cracks in welded connections and in steel plates subjected to tension. The findings are discussed in three different papers presented in the following chapter.

The use of CFRP's to prevent fatigue damage was investigated experimentally and analytically through the analysis of subassemblies representing a segment of the tension flange of a steel bridge with a welded coverplates. This type of welded connection is defined as a fatigue category E' in accordance to the AASHTO bridge design code if the weld tying the flange to the coverplate is smaller than 102 mm (4 in.), and perpendicular to the direction of the flange. The subassembly used to simulate the flange-coverplate connection was loaded under three point bending, and consequently it is referred to as a bending specimen.

Bending specimens were repaired with three different types of preventive treatments to minimize fatigue damage in the welded connections: CFRP overlays made with continuous fibers that were prefabricated under laboratory conditions, chopped-fiber sprayed overlays which were simpler to fabricate, and smoothing of the surface of the welds. The findings related to the repair methods for the bending specimens are presented in the first article.

There were several important findings from three point bending specimen study. The method of reinforcing the welded connections with the continuous fiber overlays was very effective in reducing the stress demand on the welds, driving the fatigue-crack initiation life into the infinite fatigue life range of the AASHTO design curves. The chopped fiber technique evaluated in this study is fairly new. The study showed that this technique was still limited by the bond strength of the overlay under fatigue loading. Future studies will focus on improved fabrication techniques to address this problem.

Crack propagation studies were performed both on bending specimens and is tension specimens consisting of a steel plate with a center hole. The latter type of specimen was chosen to investigate the possible use of CFRP's to repair fatigue cracks propagating through webs and flanges of plate girders.

The second study using a tension plate with a hole studied two different methods of continuous and chopped fiber. The details of the crack propagation study are presented in the second article. Specimens reinforced with continuous fiber overlays had an excellent response, extending the fatigue-crack propagation life of the specimens by more than 30 times.

The third study that was carried out was intended to provide a better understanding of the factors that affect the bond between the CFRP overlays and the steel. This study was carried out using pull-out tests of various bond layer configurations under monotonic loading. During the

development of the CFRP overlays, tests showed that the limiting factor was maintaining the bond between the composite and the steel during cyclic loading. Several improvements were made to the configuration of the bond layer to improve the strength under fatigue loading. One of the most important ones was the embedment of a layer of breather cloth within the bonding layer, which led to large improvements in fatigue life. The pull-out tests were carried out to gain a better understanding of the reasons that made the breather cloth improve the performance of the bond layer under cyclic loading. Another important finding of this study is related to the importance of using breather cloth in resin layers of different thickness. It was found that if the bond layer was thin, the bond strength was not sensitive to the embedment of the breather cloth. However, if the bond layer was thick enough, specimens with breather cloth developed bond strengths 26% higher than those without breather cloth.

USE OF CFRP OVERLAYS TO STRENGTHEN WELDED CONNECTIONS UNDER FATIGUE LOADING

Abstract

In study, the performance of various methods to prevent and repair fatigue damage in welded connections was evaluated. Fatigue is a recurring problem that affects a significant number of steel bridges in the National inventory. Results from experimental tests and analytical simulations of specimens with welded connections reinforced with carbon fiber reinforced polymer (CFRP) overlays and loaded in three-point bending are presented. Some of the specimens were reinforced with prefabricated multi-layered CFRP overlays, while others were reinforced with sprayed CFRP overlays. Specimens were tested under cyclic loading to evaluate the fatigue-crack initiation life of the welded connections reinforced with CFRP overlays. Experimental results were compared with results from similar specimens treated using other techniques to strengthen welded connections, namely Ultrasonic Impact Treatment (UIT) and weld surface smoothing. Test results showed that when bond between the CFRP overlay and the steel was maintained, the reduction in stress demand was sufficient to extend the fatigue life of the welded connections from AASHTO category E performance to the infinite fatigue life range.

It was found that bond was critical to the performance of this repair technique, and additional fatigue tests were performed to evaluate the fatigue life of the interface layer used to attach the CFRP overlays to the steel. Test results showed that the fatigue strength of the bond layer was drastically improved by introducing breather cloth material within the interface layer.

Introduction

A significant number of studies have been performed, mostly in the aerospace field, to investigate the use of Fiber Reinforced Polymers (FRP) to repair metal plates with fully developed fatigue cracks (Sabelkin et al. 2007; Schubbe et al. 1999; Tavakkolizadeh et al. 2003). In most instances discussed in the literature, pre-existing cracks or notches are covered with one or a few layers of composite sheets to effectively reduce the rate of crack growth. There are very few studies (Nakamura et al. 2009) investigating the use of composite materials to repair or strengthen welded connections. Because welded connections are very common in existing bridge structures, and because the implementation of repairs in this type of connections is often challenging due to limitations imposed by complex geometry, the use of composite materials presents a new alternative that significantly expands the tools available to bridge engineers.

In terms of linear elastic fracture mechanics theory, there are essentially three alternatives to improve fatigue life, if material properties remain the same (Barsom et al. 1999): to reduce the initial flaw size, to reduce the stress range, or to induce a residual stress field that will cause the area subjected to fatigue loading to be in compression.

Repair methods such as laser peening and ultrasonic impact treatment improve fatigue life by reducing the initial flaw size and introducing a residual stress field. Other repair techniques, such as bolting, and attachment of fiber reinforced polymer (FRP) overlays increase fatigue life by reducing the stress demand. There are many examples in the literature that show the effectiveness of FRP materials when used to repair existing notches or cracks. For example, (Tavakkolizadeh et al. 2003) concluded that the use of FRP sheets to repair notched beam flanges led to significant improvements in fatigue life. Because FRP repairs work by reducing

the stress range experienced in the metal substrate, this method should be effective before and after crack initiation, so long as bond between the FRP and the underlying metal is maintained.

Background

Several studies conducted in the past (Nakamura et al. 2009; Tavakkolizadeh et al. 2003), including recent experimental work performed at the University of Kansas on welded steel connections (Kaan et al. 2008), show that bonding FRP sheets or overlays can be a very effective technique to improve fatigue-crack initiation life and fatigue-crack propagation life in steel bridge components. This study focuses on the repair of welded cover plate connections that have thick cover plates, which are known to be vulnerable to fatigue damage (Albrecht et al. 2007), using prefabricated Carbon Fiber Reinforced Polymer (CFRP) overlays. This particular type of connection was chosen because its geometry falls within the worst fatigue category in the AASHTO LRFD Bridge Design Specification (2004), Category E', and consequently allows for the evaluation of strengthening techniques that bring about large increases in fatigue life.

A thorough review of experimental work carried out to characterize the fatigue performance of welded cover plates in steel beams, including several retrofit techniques, is presented by (Albrecht et al. 2007). Experimental data presented in this review showed that three techniques: end bolting, splicing, and bonding of the cover plates with an epoxy adhesive, resulted in large increases in fatigue life, pushing the beams to the infinite fatigue life range.

The present study is a continuation of studies carried out by (Vilhauer 2007), (Petri 2008) and (Kaan et al. 2008), evaluating the performance of various repair and retrofit measures for welded connections. (Vilhauer 2007) tested 17 steel welded cover plate specimens (Fig. 1) to

investigate the performance of several fatigue strengthening methods. The specimens used in that study each consisted of two steel plates connected all-around with an 8-mm (0.313-in.) shielded metal arc (SMAW) fillet weld. One of the plates had dimensions of 1270 mm x 114 mm x 25.4 mm (50 in. x 4.5 in. x 1.0 in.), while the other had dimensions of 660 mm x 76.2 mm x 25.4 mm (26 in. x 3.0 in. x 1.0 in.) Both plates were Grade A36 steel. The specimen was supported in the vertical direction at a distance of 76 mm (3.0 in.) from both edges of the larger plate. (Vilhauer 2007) evaluated three different fatigue strengthening methods: ultrasonic impact treatment (UIT), a post-installed fully-tensioned structural high-strength bolt, and a combination of the two techniques. Vilhauer (2007) found that specimens in which the welds were treated with UIT were able to reach infinite fatigue life when tested at a stress range of 138 MPa (20 ksi).

(Kaan et al. 2008) studied the use of CFRP overlays for increasing fatigue crack initiation life. Kaan (2008) conducted experiments with two different types of prefabricated overlays: Type I and Type II. Type I overlays were fabricated by placing successive layers of bidirectional woven carbon-fiber ply until the desired geometry was achieved. Type II overlays were developed to obtain greater consolidation and uniformity than achieved in Type I overlay elements. Type II overlays were comprised of 36 plies of bidirectional woven carbon fiber plies (pre-impregnated with cyanamide-123 resin) and four plies of boron fiber, and were more uniform and more highly consolidated than Type I overlays. In testing that utilized Type I overlays, fatigue failure occurred through the composite material, instead of the bond layer or the welded connection.

Four fatigue tests were conducted by Kaan (2008) using Type II CFRP overlays, and the results are presented in Table 1. Although the fatigue crack initiation life of the steel substrate

increased, repeated bond failures between the CFRP and the steel occurred. When debonding of the overlay occurred, the specimen was subjected to fatigue cycles in the unreinforced configuration until debonding was noticed through inspection; in these cases, the CFRP overlay was reattached to the steel specimen after subsequent inspection for cracks.

Table 1 : Experimental results of three point bending performed by Kaan (2008) and Vilhauer (2007)

Treatment	Specimen ID	Stress Range, Mpa (ksi)	Resin Thickness, mm (in)	Duration of test, No. of cycles	No. of cycles to crack initiation	Average number of cycles to CFRP No. of debonds	Reference:
CFRP	TRI 02	137.9 (20)	0.76 (0.03)	460,000	460,000	275,000	1 Kaan (2008)
CFRP	TRI 06	137.9 (20)	1.65 (0.065)	2,157,500	N/A	431,500	5 Kaan (2008)
CFRP	TRI 04	137.9 (20)	3.18 (0.125)	1,359,600	1,332,000	226,600	6 Kaan (2008)
CFRP	TRI 05	137.9 (20)	6.35 (0.25)	1,205,000	N/A	1,205,000	1 Kaan (2008)
None	Cntrl_03	137.9 (20)			500,000		Vilhauer (2007)
None	Cntrl_05	137.9 (20)			350,000		Vilhauer (2007)
UIT	Uit_02	137.9 (20)			5,000,000		Vilhauer (2007)

After multiple debonding failures, the steel substrate was subjected to a significant number of load cycles in the unreinforced configuration, placing it at greater risk for developing a fatigue crack. For this reason, these tests provide meaningful information about the fatigue life of the bond layer under the various configurations that were tested and also show that use of the overlays leads to an increase in the fatigue-crack initiation life of the welded connection; however, the tests do not present an appropriate measure of the magnitude of the increase in fatigue life of the welded connection if bond between the CFRP overlay and the steel substrate is maintained throughout the test.

The two main conclusions from the tests performed by (Kaan et al. 2008) were that the use of CFRP overlays led to an increase in fatigue-crack initiation life of the welded connection, and that maintaining the bond between the CFRP and the steel substrate was a critical factor to achieving the largest possible increase in fatigue-crack initiation life.

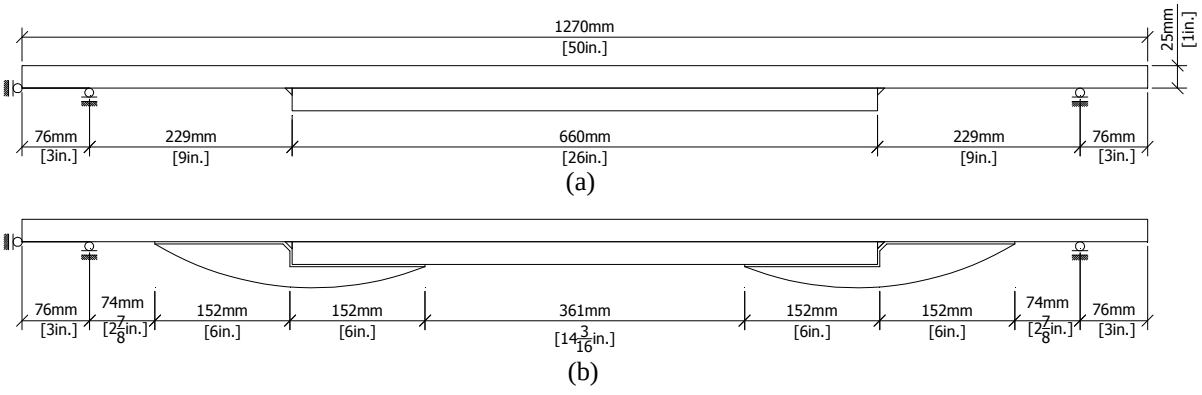

Figure 1 : Three point bending specimens: (a) Without CFRP retrofit (Vilhauer 2007); (b) With CFRP retrofit applied (Kaan 2008)

Objective

The primary objective of this study was to investigate the effectiveness of CFRP overlays as a fatigue strengthening method (attaching overlays before crack initiation) for welded connections, and to compare its effectiveness to that of other methods used to strengthen welded connections. A second objective was to determine the effectiveness of CFRP overlays in reducing fatigue crack propagation rate when used as a repair method (attaching overlays after crack initiation).

To meet both objectives, three point bending welded cover plate specimens were tested in fatigue under a constant stress range. Pre-fabricated CFRP overlays were bonded to the ends of the cover plates both prior to loading and after fatigue cracks were observed in the welds.

Finite element analyses were performed to gain a better understanding of the stress field in the region surrounding the weld toe, and how the stress range demand is affected by the configuration and geometric characteristics of the overlay.

Finite Element Simulations

The stress distribution in specimens tested by (Vilhauer 2007) and (Kaan et al. 2008) was studied by (Petri 2008) with 3D analyses performed using the finite element software ABAQUS V.6.8 (Simulia 2008). Models were created using linear elastic material models for the steel and composite materials, and a mesh consisting of 20-node brick elements. The analyses showed that attaching CFRP overlays to a welded steel cover plate connection would result in a significant reduction of peak stress at the toe of weld, which was consistent with the increase in fatigue life observed experimentally by Kaan (2008).

Deflected shapes and computed maximum principal stresses under the peak load from the various computational models analyzed by Petri are shown in Fig. 2. The stress fields show that the composite doublers are effective in reducing the high stress gradients that occur at the weld toe of the unreinforced specimen, and in distributing those stresses over a much greater area. Examination of Fig. 2 also shows that the edge of the CFRP overlay has a high stress demand, and that this point is of critical importance to maintain the bond between the FRP overlay and the substrate steel.

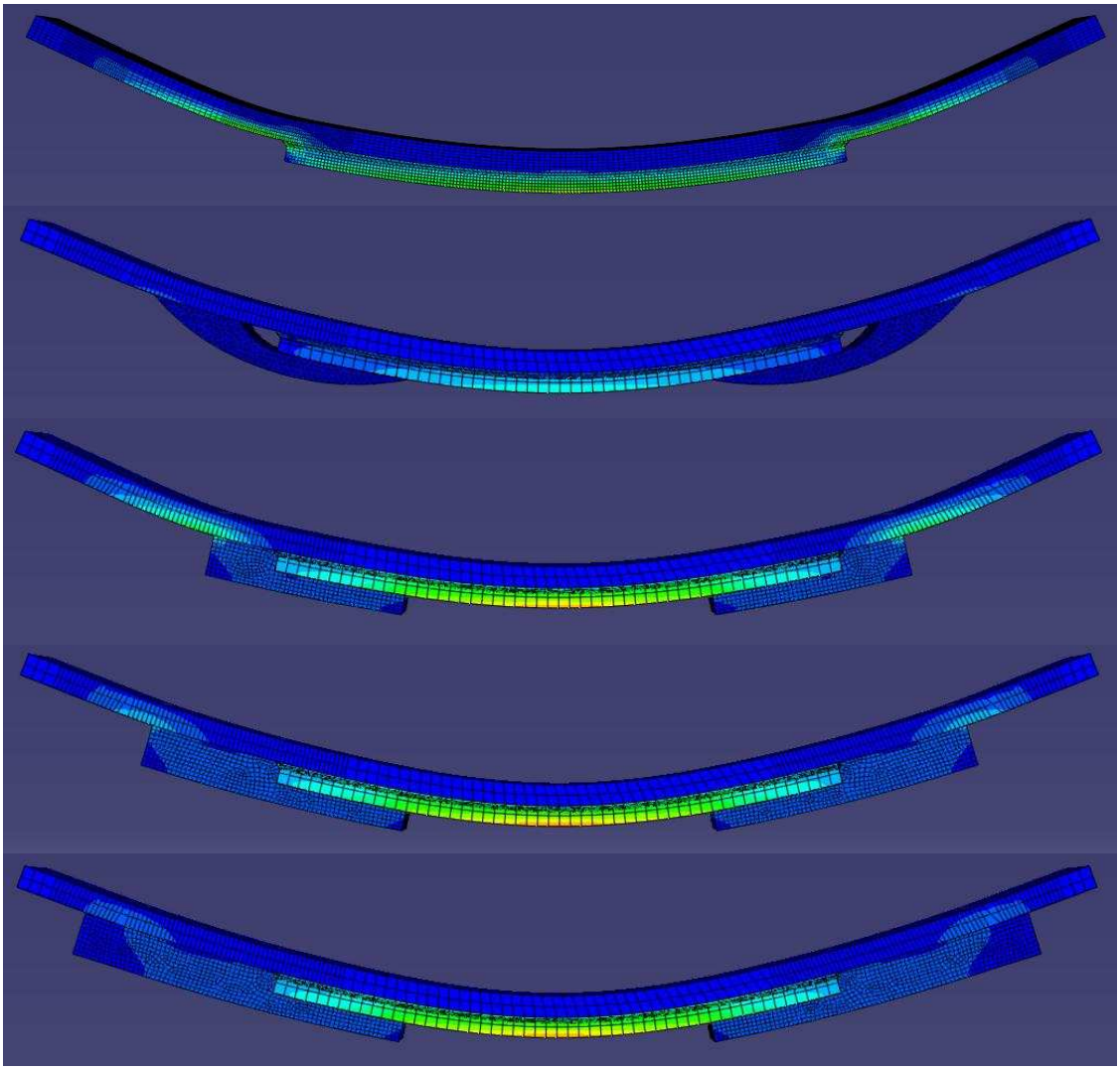

Figure 2 : Elevation view showing maximum principal stress: (a) control specimen; (b) specimen with smooth-shaped composite overlay; (c) short rectilinear composite overlay; (d) rectilinear composite overlay; (e) long rectilinear composite overlay

Additional finite element simulations were conducted as a part of this study. 2D finite element models were developed in ABAQUS v.6.8.2 (Simulia 2008) using linear elastic material properties and 4-noded plane strain elements. The 2D model captured a 25 mm (1.0 in.) mid-

width strip of the specimen. Twenty different models were analyzed to provide the basis for a parametric study. Parameters investigated included the geometric profile of the overlay, its length, thickness (Fig. 3), modulus of elasticity of the CFRP, thickness of the resin layer used to attach the CFRP overlay to the steel surface, and the presence of an unbonded region (gap) in the direct vicinity of the weld. The different geometric profile parameters that were investigated are shown in Fig. 3.

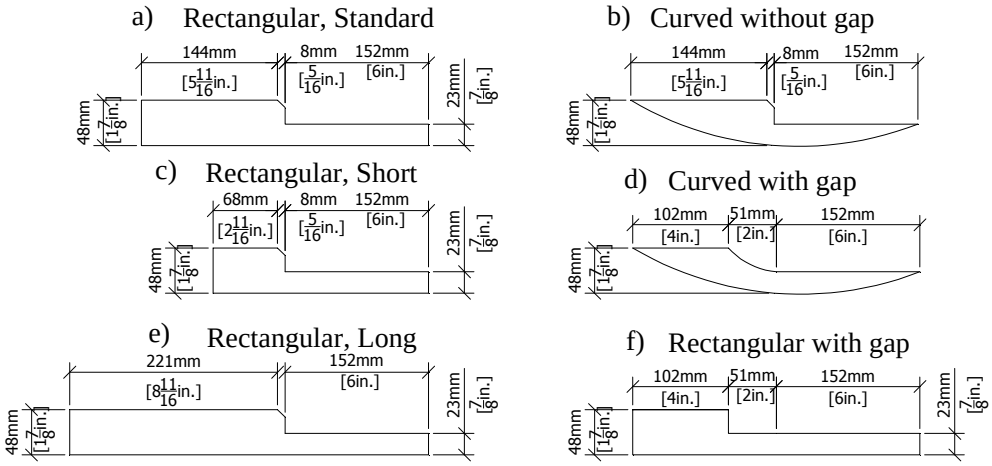

Figure 3 : Different configuration of CFRP overlay evaluated in the analytical model

The parametric study was intended to determine the optimum configuration of the CFRP overlay and to investigate how effective the overlay could be expected to be in decreasing the peak stress demand at the weld toe. Computed stress fields in the vicinity of the weld for the unreinforced and reinforced (Fig. 3b) configurations are presented in Fig. 4. The 2D simulation results were consistent with those obtained by Petri (2008) in that addition of the overlay resulted in a significant reduction in the peak stress demand at the weld toe (on the order of 80% for the

overlay configuration shown in Fig 3d). These simulation results were also consistent with the increments in fatigue life increase observed by Kaan et al. (2008).

The suite of Finite Element simulations performed in this study evaluated the effect of the following parameters: geometric configuration of the overlay, thickness of the interface bond layer, and the modulus of elasticity of the composite.

The 2D simulations showed that the geometric profile of the CFRP overlay did not have a significant effect on the calculated stress demand at the weld toe, whereas the presence of a gap between the weld and the CFRP overlay did have a notable effect. This is illustrated in Figs. 5 and 6, which present the computed longitudinal stress along a path on the surface of the bottom steel plate. The observed trends in the calculated longitudinal stress and the maximum principal stress were similar in nature, so the directional stress presented in the figures was chosen on the basis of clarity.

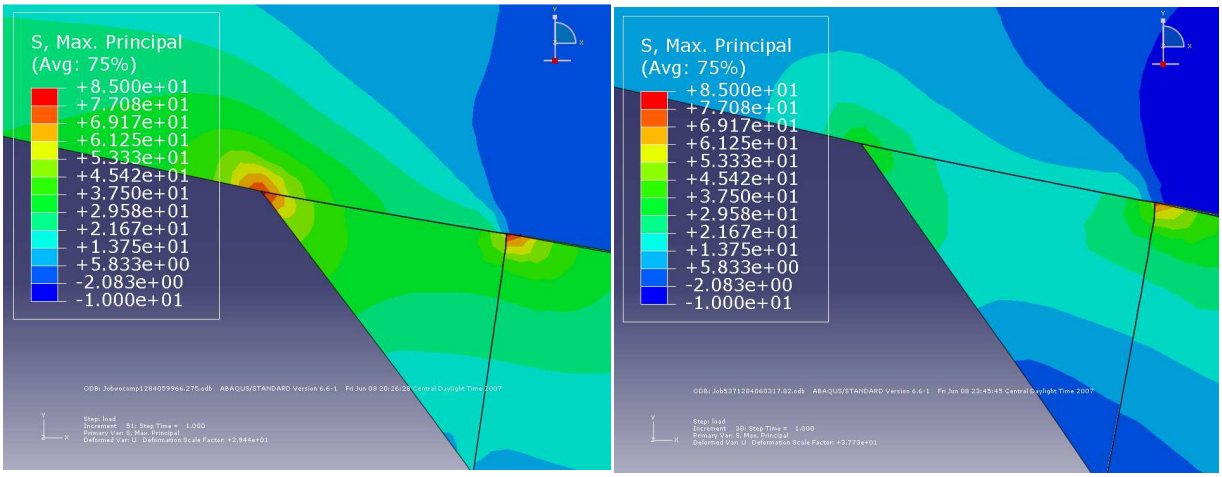

Figure 4 : Elevation view showing maximum principal stress: (a) control specimen; (b) specimen with smooth-shaped composite overlay.

In Figs. 5 and 6, the spike in stress observed at a distance of approximately 298 mm (11.8) in. from the edge of the specimen corresponds to the location of the toe of the weld, while the back of the weld was located at approximately 307 mm (12.1 in.) from the edge of the specimen.

Figure 5 shows that a curved and a rectilinear CFRP overlay configuration were equally effective in reducing the peak stress demand at the toe of the weld. Figure 6 shows that the most effective retrofit scheme involved bonding the overlay up to the location of the weld, which resulted in a reduction on the peak stress demand at the weld toe on the order of 80%. When the analysis was performed leaving a gap near the weld toe (configuration shown in Fig. 3d) the reduction in peak stress demand at the weld toe was still very significant, on the order of 60%, but the efficiency of the repair was diminished.

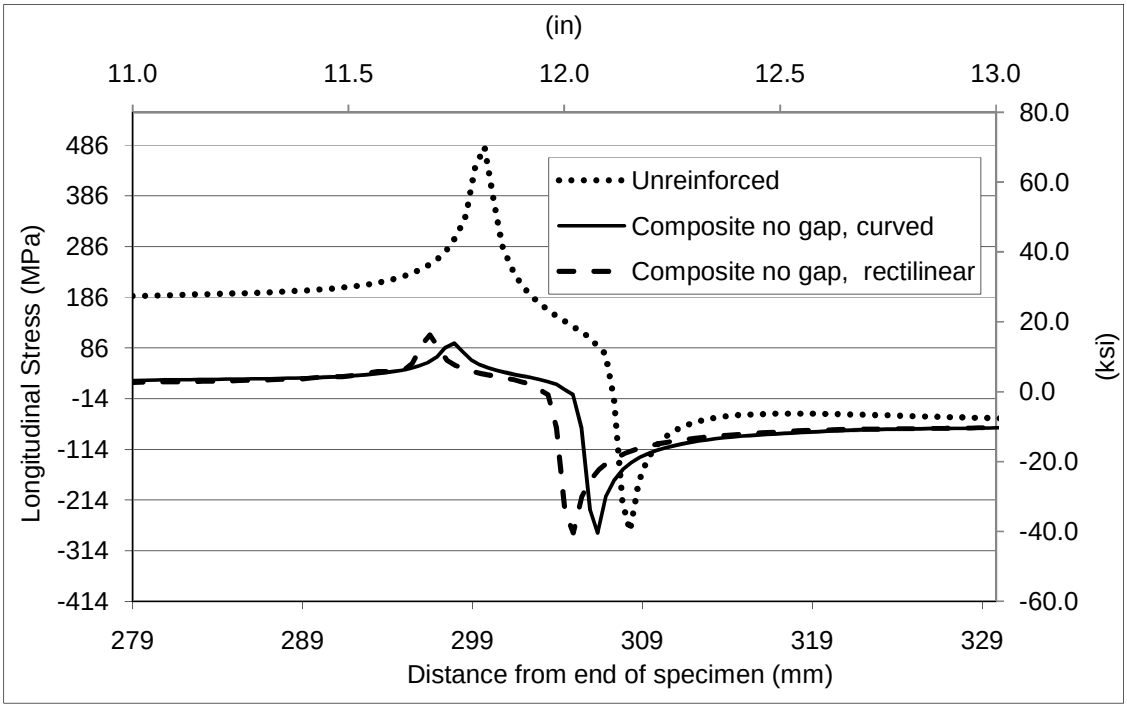

Figure 5 : Effect of composite overlay shape on longitudinal stresses in the area of the weld

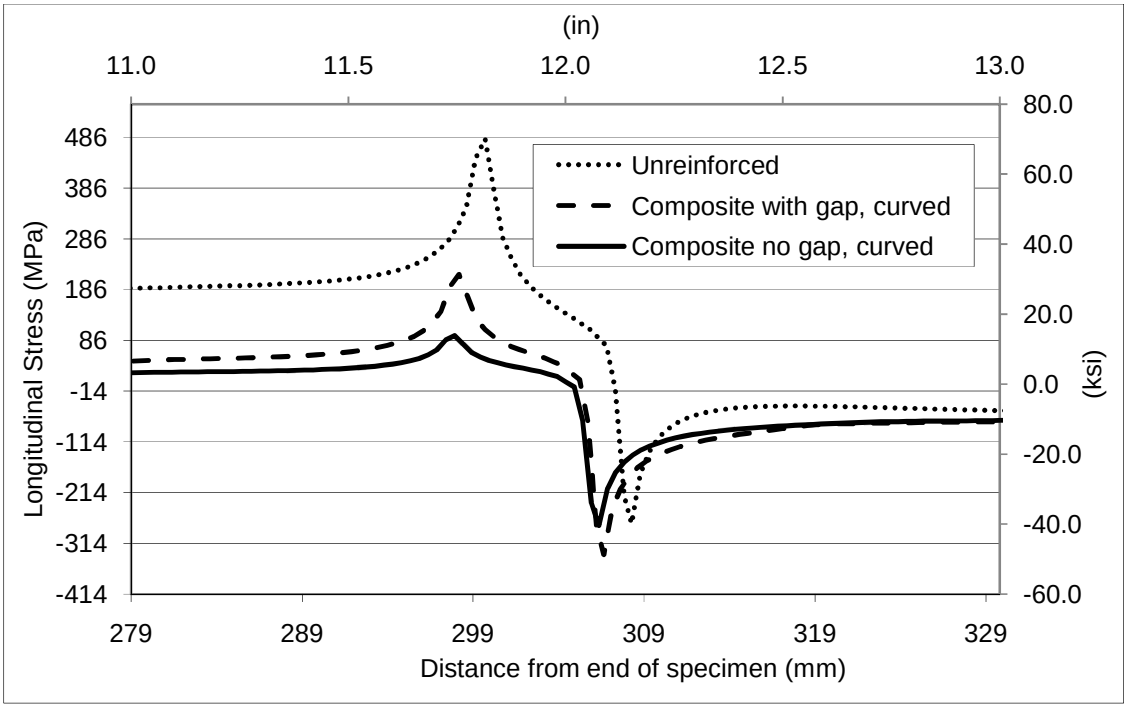

Figure 6 : Effect of composite overlay shape on longitudinal stresses in the area of the weld

The analyses showed that within the evaluated range of values, other parameters related to the shape of the CFRP overlay, such as length and the thickness of the overlay, did not significantly affect stress demand at the toe of the weld.

Of the remaining parameters, the modulus of elasticity of the composite and the thickness of the interface bond layer had the most significant effect on the stress demand at the weld toe. The effect of the modulus of elasticity of the CFRP overlay is illustrated in Fig. 7. A reference value of 26.6 GPa (3,860 ksi) was adopted for the modulus of elasticity based on experimental measurements performed on the composite material used to fabricate the overlays used in this study. A suite of FE analyses were performed in which the CFRP modulus of elasticity ranged

between 60% of the reference value (16 GPa [2,315 ksi]) and 400% of the reference value (106 GPa [15,430 ksi]). Results presented in Fig. 7 are for the overlay configuration shown in Fig. 3b. Figure 7 shows that increasing the modulus of elasticity of the CFRP overlay results in diminishing returns. These results suggest that prefabricating the overlay to achieve higher fiber contents leads to a greater increase in fatigue life of the welded connection, and also suggest that, for the analyzed overlay configurations, paying a premium for very stiff fibers may not bring about a meaningful increase in fatigue life beyond that achievable with conventional fibers.

The effect of the thickness of the interface layer is illustrated in Fig. 8, which shows that explicitly modeling the flexibility of the interface layer resulted in a lower stress demand at the weld toe. When the interface layer was modeled, increasing the thickness of the overlay resulted in a slight increase in the peak stress demand at the weld toe. This indicates that a thicker interface layer is less effective in reducing the peak stress demand at the weld toe than a thinner interface layer. However, the analyses also showed that peak shear and peel stress demands at the interface between the composite and the bond layer exhibited the opposite trend. Fig. 9 shows that as the thickness of the interface decreased (which reduces the calculated stress demand at the weld toe), both the calculated peak shear and peel stress demands increased, which can be expected to have a detrimental effect on bond strength under cyclic loading.

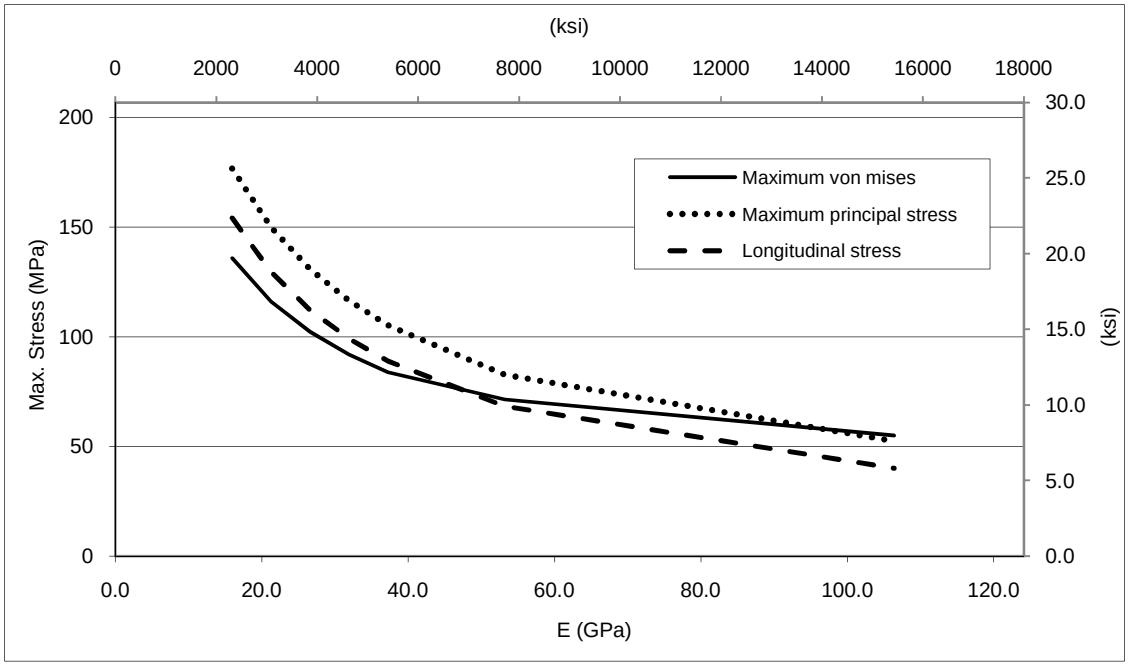

Figure 7 : Effect of composite overlay stiffness on maximum stress demand at the wed toe

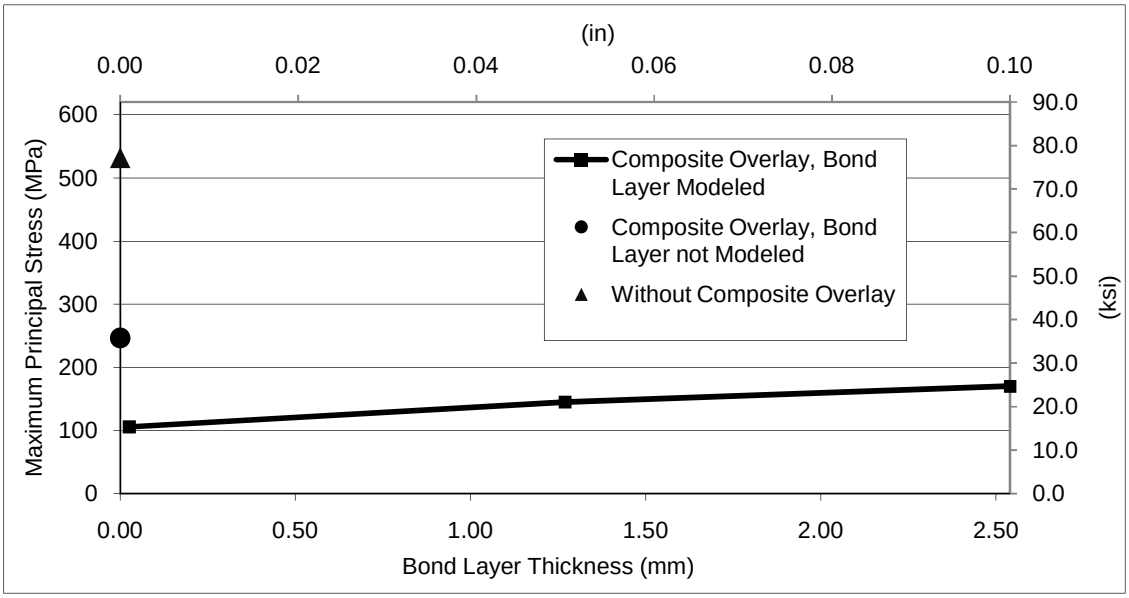

Figure 8 : Maximum principal stress on the steel plate in the vicinity of the weld overlay stiffness on maximum stress demand at the weld toe

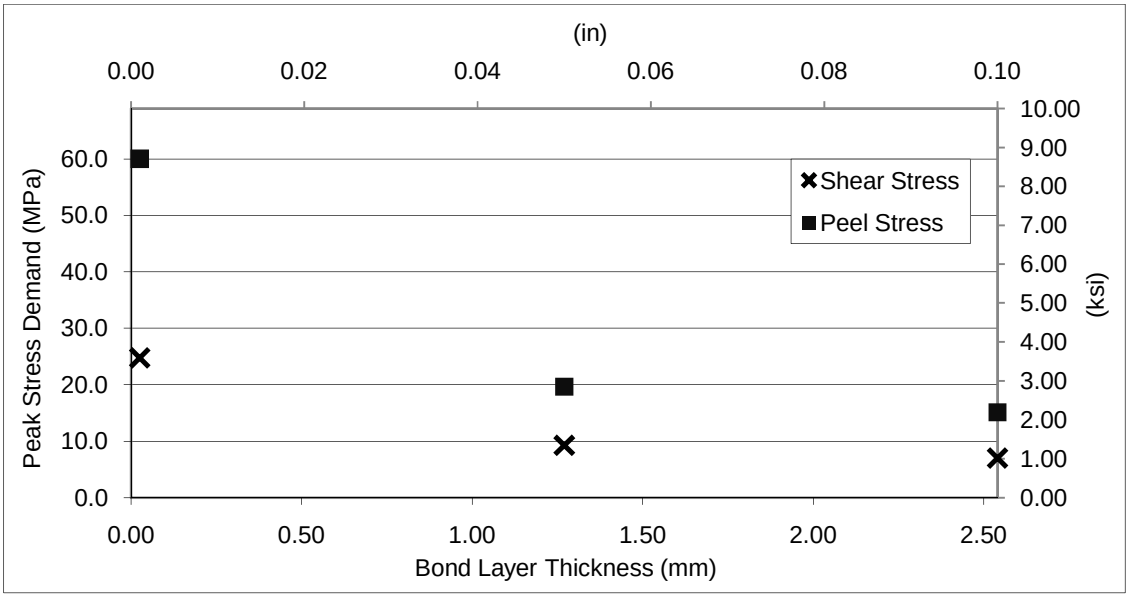

Figure 9 : Maximum stress demand at the interface between the composite and the bond layer

Experimental Analysis

The experimental program consisted of a series of welded cover plate specimens loaded in three point bending and subjected to cyclic loading under a constant stress range (Fig. 1). The three point bending specimens were comprised of two plates with identical dimensions as those studied by Vilhauer (2007) and Kaan et al. (2008), and previously described. The specimens were restrained from vertical motion at points 76 mm (3.0 in.) from the edges of the larger plate. The smaller plate was attached to the larger plate with a continuous 7.9 mm ($^{5}/_{16}$ in.) fillet weld all around the perimeter of the smaller plate.

The experimental matrix is summarized in Table 2. As shown, three different types of treatments were utilized, including three different types of composite overlays. To establish a frame of reference based on the type of geometric discontinuity, the welded connection between

the two plates was classified as an AASHTO Category E' detail (AASHTO 2004). According to the AASHTO design curves, the nominal stress range for a Category E' detail should be maintained below 31.0 MPa (4.50 ksi) in the area of the weld to ensure that cracking will not initiate under fatigue loading. Loads were selected to achieve a high stress range of 138 MPa (20.0 ksi) at the transverse welds, at the location of the weld toes. The ratio of maximum to minimum load was selected as $R = 0.10$. The maximum load was 17.1 kN (3.84 kips) and the minimum load was 1.70 kN (0.38 kips).

Three specimens were strengthened with prefabricated multi-layered CFRP overlays, and were designated TRI 04, TRI 06, and TRI 07. Multi-layered CFRP overlays were prefabricated following the same procedure used by Kaan (2008) for Type II overlays. The dimensions of CFRP overlay were 300 mm x 76 mm x 38 mm (12 in. x 3.0 in. x 1.5 in). The shape of CFRP was curved in profile, without leaving any gap between weld and the CFRP (Fig. 3b). Breather cloth approximately 2.4 mm (0.09 in.) thick was embedded within the resin layer to improve bond behavior under cyclic loading.

Of the three specimens treated with muli-layered CFRP overlays, two (TRI 06 and TRI 07) were intended to study the effectiveness of CFRP overlays for preventing fatigue damage in the area near the weld toe. The remaining specimen (TRI 04) was used to investigate the effectiveness of the CFRP overlays to repair a connection with a pre-existing fatigue crack in the weld. One of the uncracked specimens (TRI 07) had never been loaded before, while the other two specimens (TRI 04 and TRI 06) had already been subjected to fatigue loading by Kaan (2008).

In addition to the specimens described above, three specimens were treated with chopped fiber overlays. The chopped fiber overlays were fabricated using an external mixing spray

machine (a non-atomized resin LEL chopper system commercialized by BINKS). The spray machine utilized a vinyl ester resin with Norox MEKP-925 catalyst and graphite fiber yarn. Prior to spraying the composite material, the surface of the steel substrate was abraded using an angle grinder and cleaned with acetone and isopropyl alcohol. After cleaning, the fiber-resin mix was sprayed in layers approximately 3.2 mm (0.13 in.) thick and compacted using a hand tool until the outer shape of the composite overlay was similar to that of the multi-layered CFRP overlay (Fig. 3b). The specimen was cured at room temperature for two days, after which the remnant resin was cleaned from the steel substrate. In the specimen designated CHP 2, a breather cloth layer was placed on the surface of the steel and saturated with resin before spraying the combined resin-chopped graphite fiber mix. In the specimen designated CHP 3, the breather cloth was soaked with Hysol® resin and cured for two hours at room temperature before a resin-chopped glass fiber mix was sprayed.

Table 2 : Experimental matrix

Specimen ID	Stress Range MPa (ksi)	Thickness of Bond Layer with Breather Cloth mm (in.)	Treatment Type	Fiber Type
TRI 04	138 (20)	6.4 (0.25)	CFRP Overlay	Carbon
TRI 06	138 (20)	6.4 (0.25)	CFRP Overlay	Carbon
TRI 07	138 (20)	3.2 (0.125)	CFRP Overlay	Carbon
CHP1	138 (20)	None	Chopped Fiber	Carbon
CHP2	138 (20)	6.4 (0.25)	Chopped Fiber	Carbon
CHP3	138 (20)	6.4 (0.25)	Chopped Fiber	Glass
GRND 1	193 (28)		Smoothed Weld	
GRND 2	193 (28)		Smoothed Weld	
GRND 3	193 (28)		Smoothed Weld	
GRND 4	193 (28)		Smoothed Weld	
Control (TRI 08)	138 (20)			

Table 3 : Material test results

CFRP

Number of Layers in Coupon	Number of Coupons	Avg Modulus of Elasticity GPa (ksi)	Standard Deviation GPa (ksi)
1	3	85.8 (12,438)	10.0 (1,445)
3	4	75.3 (10,926)	10.9 (1,581)
5	3	61.7 (8,944)	0.3 (42)
9412 Hysol® Resin			
Coupon Thickness mm (in.)			
6.4 (0.25)	6	2.1 (303)	0.2 (25)
Chopped fiber (Carbon Fiber)			
Coupon Thickness mm (in.)			
4.8 (0.19)	7	14.1 (2,052)	6 (866)
Chopped fiber (Glass Fiber)			
Coupon Thickness mm (in.)	5	7.2 (1044)	0.5 (77)

All other specimens tested were not treated with composite overlays. An additional control test (TRI 8) was performed to complement the data set developed by Vilhauer (2007) on identical specimens (Table 1). The remaining specimens without overlays (GRND 1 through GRND 4) were treated by smoothing out the roughness of the surface of the welds using an angle grinder. When the smoothing process was finished, the surface of the weld was approximately flat, and formed an angle of approximately 45 degrees with respect to the surface of both plates. After grinding, the surface of the weld was cleaned with a steel brush to ensure imperfections from the welding process had been removed. This process was repeated until no imperfections were visible. The two goals of the weld treatment were to ensure that there was a smooth

transition between the weld and the plate at the weld toe, and to significantly reduce the initial size of the weld flaws created during the welding process.

Measured material properties are presented in Table 3. Coupon tests performed in accordance with ASTM 3039/D 3039M (ASTM 2000) from single-layered specimens showed that the modulus of elasticity of the CFRP was approximately 83 GPa (12,000 ksi). The modulus of elasticity of the 9412 Hysol® resin and of the chopped fiber composite were also measured using coupon tests (Table 3) as prescribed by ASTM 3039/D 3039M (ASTM 2000). The measured modulus of elasticity of the resin was 2.1 GPa (300 ksi).

The stress-strain relationship for the steel is presented in Fig. 10. The yield strength of the steel was found to be 300 MPa (43 ksi), and the tensile strength was 490 MPa (70.9 ksi).

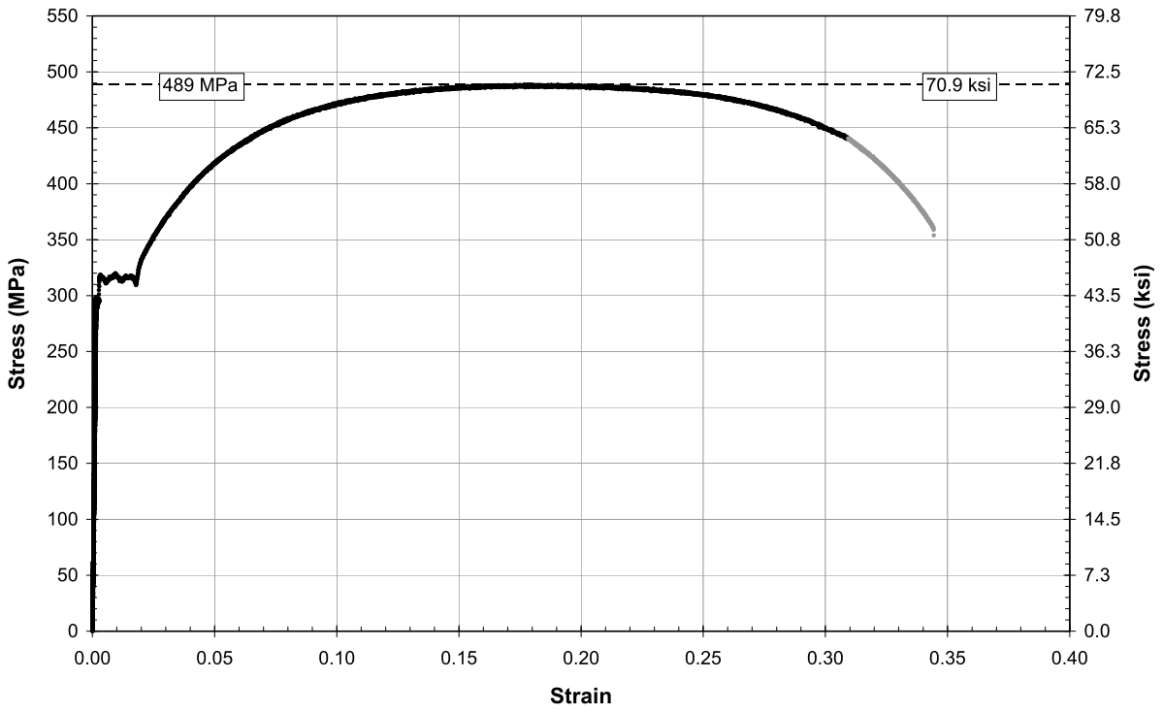

Figure 10 : Stress strain curve for the steel

Pull-out Tests

As shown in Table 2, five out of the six specimens treated with composite overlays were fabricated to have breather cloth in the interface resin layer between the steel and the composite. The effects of using breather cloth were further investigated through a series of pull-out tests carried out to complement the fatigue experimental program. The breather cloth used in this study was white polyester fiber mesh with the appearance of felt fabric. Two different types of pull-out tests were performed. The first test setup was comprised of a CFRP overlay and a steel plate similar to the configuration used in the three-point bending fatigue tests.

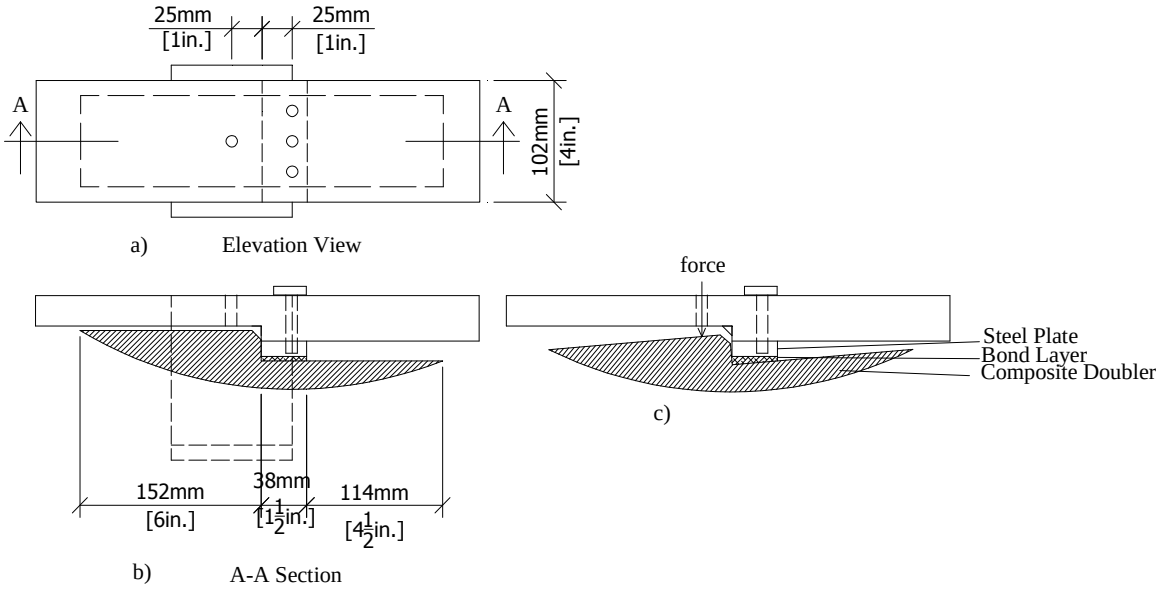

Figure 11 : Pull-out test fixture (a,b) pull-out test procedure (c)

The pull-out test fixture consisted of a steel plate with dimension of 38 mm x 100 mm x 13 mm (1.5 in. x 4.0 in. x 0.50 in.) and a 25 mm-diameter (1.0 in.) hole located 25 mm (1.0 in.) from the center of the fixture (Fig. 11a). The plate was bolted to a steel box and the load was applied to the CFRP with a pin that was pushed through the 25 mm-diameter (1.0 in.) hole with a load frame (Fig. 4c). The observed mode of failure observed in these tests was delamination of

the CFRP overlay, instead of failure in the bond layer. For this reason, all subsequent tests were performed using a second steel plate instead of CFRP overlay, so that bond strength characteristics could be ascertained directly. This second steel plate had a dimension of 178 mm x 95.3 mm x 12.7 mm (7.00 in. x 3.75 in. x 0.50 in.). The experimental matrix and results from the second series of pull-out tests are summarized in Table 4.

Table 4 : Pull-out test results

Number of tests	Thickness of resin layer mm (in.)	Breather Cloth (y/n)	Avg. Peel Stress (MPa [psi])
2	1.6 (0.0625)	n	4.62 (669.4)
2	1.6 (0.0625)	y	4.56 (661)
3	3.2 (0.125)	n	3.16 (458)
3	3.2 (0.125)	y	3.70 (536)
2	6.4 (0.25)	n	2.23 (323)
2	6.4 (0.25)	y	2.81 (408)

Results from Three-point Bending Specimens under Fatigue Loading

There were two distinct modes of fatigue failure observed in the tests carried out by Vilhauer (2007), Kaan (2008) and those performed as part of this study: fatigue failure of the bond layer between the composite and the steel, and fatigue failure of the welded connection. For this reason the results are interpreted in terms of two different types of fatigue tests, those related to the fatigue life of the bond layer (Table 5), and those related to the fatigue life of the welded connection (Table 6).

Fatigue Strength of the Bond Layer

The study by Kaan (2008) showed that composite overlays can effectively prevent fatigue failure of the welded connection, but to do so, it is essential to avoid failure of the bond layer due to fatigue. The effect of various bonding techniques on the fatigue strength of the bond layer are

shown in Fig. 12, and test results are summarized in Table 5. Designations for the experiments carried with multi-layered CFRP overlays were defined in terms of the thickness of the bond layer because overlays were reattached to the same cover plate specimen multiple times. Specimens without breather cloth (tested by Kaan [2008]) are designated by the letter C, those with breather cloth (tested as part of this study) are designated BC, and the three specimens with chopped fiver overlays (also tested as part of this study) are designated by the letters CHP. The number in the designation of specimens with multi-layered overlays represents the thickness of the bond layer in units of in. x 10^4.

The results show that all specimens with multi-layered overlays that were bonded using breather cloth achieved run-out at a very high stress ranges without failure of the bond layer. This is in direct contrast to the tests carried out by Kaan (2008) without breather cloth. For example, a fatigue test reported by Kaan (2008) performed on a steel specimen with CFRP bonded to it without breather cloth cycled 1.33 million cycles before crack initiation; however, the CFRP doubler debonded six times during the test. Each time a debonding occurred, the CFRP overlay was completely removed from the specimen and rebonded. The thickness of the resin layer was 3.2 mm ($^1/_8$ in.). Fatigue tests performed utilizing breather cloth embedded in the resin bond layer of the same thickness (3.2 mm [$^1/_8$ in.]) sustained 3.3 million cycles without any observed debonding between the CFRP and steel. After 1.5 million cycles, the CFRP overlay was removed, and the steel substrate was inspected for cracks. No cracks were discovered.

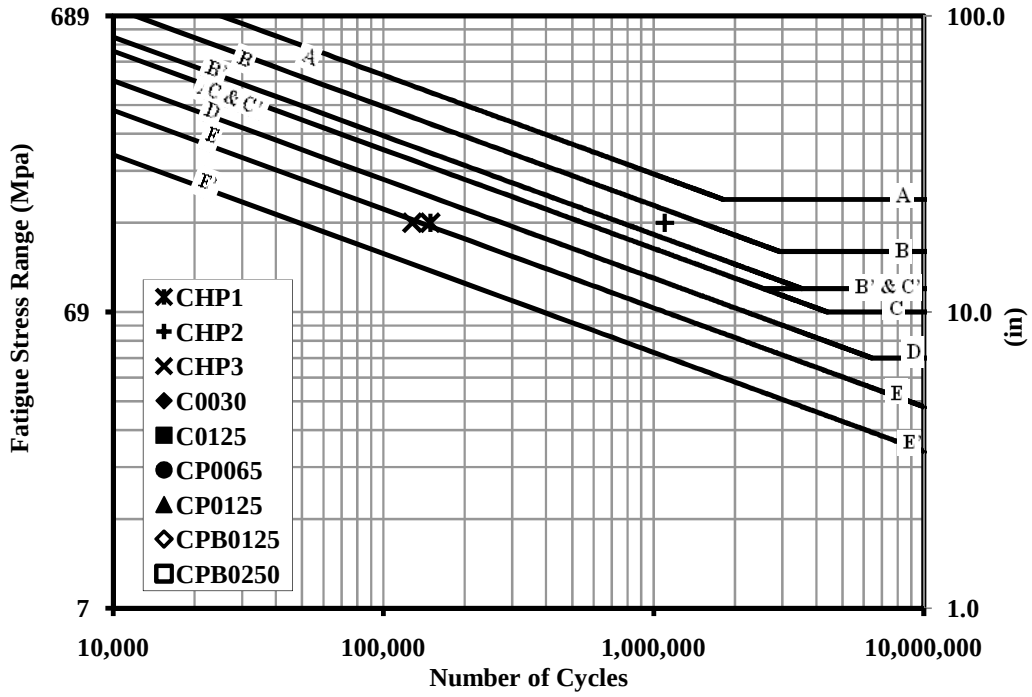

Figure 12: Fatigue Life of Bond Layer for various Bonding Techniques

In specimens without breather cloth the average fatigue life of the bond layer with a thickness of 1.6 mm (0.06 in.) was 431,000 cycles, while the average fatigue life for bond layers with a thickness of 3.18 mm (0.13 in.) was 216,250 cycles. The coefficients of variation were 0.51 and 0.75, respectively. The scatter of the results can be appreciated in Fig. 12. The fact that the trend opposes the results from the Finite Element Analysis was indicative that fabrication problems induced significant variability in the results and severely affected the fatigue life of the bond layer.

Table 5 : Fatigue Life of bond layer for various bonding techniques

Test Designation	Stress Range, Mpa (ksi)	Resin Layer Thickness, mm (in.)	Number of Cycles to Bond Failure
C0030-01	137.9 (20)	0.762 (0.0300)	275,000
C0030-02	137.9 (20)	0.762 (0.0300)	900,000
C0125-01	137.9 (20)	3.175 (0.1250)	529,800
C0125-02	137.9 (20)	3.175 (0.1250)	255,750
C0125-03	137.9 (20)	3.175 (0.1250)	134,150
C0125-04	137.9 (20)	3.175 (0.1250)	71,150
C0125-05	137.9 (20)	3.175 (0.1250)	204,500
C0125-06	137.9 (20)	3.175 (0.1250)	1,125,300*
CP0125-01	137.9 (20)	3.175 (0.1250)	1,060,950*
CP0125-02	137.9 (20)	3.175 (0.1250)	722,000*
CPB0250-03	137.9 (20)	6.350 (0.2500)	1,318,900*
CPB0250-04	137.9 (20)	6.350 (0.2500)	1,318,900*
CPB0250-05	137.9 (20)	6.350 (0.2500)	1,547,850*
CPB0250-06	137.9 (20)	6.350 (0.2500)	1,547,850*
CP0065-01	137.9 (20)	1.588 (0.0625)	279,750
CP0065-02	137.9 (20)	1.588 (0.0625)	283,900
CP0065-03	137.9 (20)	1.588 (0.0625)	802,900
CP0065-04	137.9 (20)	1.588 (0.0625)	153,706
CP0065-05	137.9 (20)	1.588 (0.0625)	637,846
CPB0250-07	137.9 (20)	6.350 (0.2500)	1,550,450*
CPB0250-08	137.9 (20)	6.350 (0.2500)	1,550,450*
CPB0250-01	137.9 (20)	6.350 (0.2500)	1,205,315
CPB0250-02	137.9 (20)	6.350 (0.2500)	1,634,756*
CPB0125-01	137.9 (20)	3.175 (0.1250)	1,725,900*
CPB0125-02	137.9 (20)	3.175 (0.1250)	1,725,900*
CPB0125-03	137.9 (20)	3.175 (0.1250)	1,564,300*
CPB0125-04	137.9 (20)	3.175 (0.1250)	1,564,300*

**Test was stopped without observed debonding after number of cycles exceeded infinite fatigue life*

Of the three specimens reinforced with chopped fiber overlays, the best results were obtained with test CHP2, in which a layer of breather cloth was first saturated with the

same resin used in the chopped fiber composite, and later sprayed with the resin-fiber mix. Test CHP1, in which the chopped fiber mix was sprayed directly on the steel surface, had very weak bond strength under fatigue loading. This was also the case for test CHP3, in which a layer of Hysol® with embedded breather cloth was adhered to the steel prior to spraying with the resin-fiber mix. In this case, failure occurred at the interface between the Hysol® and the sprayed fiber composite.

Fatigue Crack Initiation Life of the Welded Connections

The tests performed with breather cloth in the bond layer showed that by implementing this fabrication technique the bond layer could achieve run-out under very high applied stress range. Having addressed the bond problem under fatigue loading, the remaining research problem was whether the reduction in stress demand afforded by the composite overlays would be sufficient to extend the fatigue life of the welded connections to the infinite range, as suggested by the results from the Finite Element Analysis. To address this question, two specimens were strengthened with CFRP overlays using breather cloth within the resin layer. The first, designated as TRI 06 in Tables 2 and 6, had been previously loaded with 2.1M cycles without developing observable fatigue cracks (Kaan, 2008). Testing conducted during the initial 2.1M cycles included a resin layer 1.6 mm (0.063 in.) thick, without breather cloth. Subsequent testing performed on TRI 06 used a resin layer 6.4 mm (0.25 in.) thick with breather cloth embedded within the bond layer. The specimen was tested under fatigue loading with the same protocol described in Kaan (2008). After 1.55M cycles, the test was stopped, and the composite overlay removed to inspect the weld for crack initiation. No cracks were observed.

The second specimen, designated TRI 07, was treated with a CFRP overlay and breather cloth and had not been loaded prior to this study. The thickness of the resin layer was 3.2 mm (0.13 in.) and it had embedded breather cloth. This specimen was subjected to the fatigue loading protocol for a total of 3.29M cycles. After first 1.50M cycles, the test was paused and the overlays were removed to inspect for fatigue cracks. After inspection, the overlays were reattached and the specimen loaded until a total of 3.29M cycles were reached. The final inspection showed that the specimen had not developed any detectable fatigue cracks.

To gage the effectiveness of the CFRP overlay repair technique, results from specimens reinforced with composite overlays were compared with improvements in fatigue life associated with other repair techniques evaluated using the same type of specimens. Results are summarized in Table 6 and presented in Fig. 13. Specimens that were treated by smoothing of the welds are designated GRND, specimens in which the welds were treated with UIT are designated UIT, and control specimens are designated Cntrl.

Table 6 : Experimental results of three point bending tests

Specimen ID	Stress Range MPa (ksi)	Bond Thickness mm (in)	Number of Cycles	No of Cycles to Crack initiation	Operator
TRI 02	137.9 (20.0)	0.76 (0.03)	900,000	N/A	
TRI 04	137.9 (20.0)	3.18 (0.13)	4,918,550	N/A	
TRI 05	137.9 (20.0)	6.35 (0.25)	1,634,756	N/A	
TRI 05	137.9 (20.0)	6.35 (0.25)	1,634,756	N/A	
TRI 06	137.9 (20.0)	1.59 (0.06)	3,105,106	N/A	
TRI 06	137.9 (20.0)	1.59 (0.06)	3,105,106	N/A	
TRI 07	137.9 (20.0)	3.18 (0.13)	3,290,200	N/A	
TRI 07	137.9 (20.0)	3.18 (0.13)	3,290,200	N/A	
TRI 08	137.9 (20.0)			355,450	
GRND 1	193.1 (28.0)			391,000	
GRND 2	193.1 (28.0)			1,200,000	
GRND 3	193.1 (28.0)			950,000	
GRND 4	193.1 (28.0)			600,000	
UIT 02	193.1 (28.0)			1,300,000	Vilhauer (2007)
UIT 03	193.1 (28.0)			2,100,000	Vilhauer (2007)
UIT 01	137.9 (20.0)		5,000,000	N/A	Vilhauer (2007)
Cntrl_05	193.1 (28.0)			80,000	Vilhauer (2007)
Cntrl_06	193.1 (28.0)			50,000	Vilhauer (2007)
Cntrl_04	137.9 (20.0)			350,000	Vilhauer (2007)

On average, control specimens tested at a stress range of 193 MPa (28 ksi) had a fatigue-crack initiation life of 65,000 cycles. Specimens with smoothed welds tested at the same stress range had an average fatigue life of 785,250 cycles with a coefficient of variation of 0.46. This weld treatment technique resulted in a very significant increase in fatigue life, on average raising the fatigue performance from that consistent with an AASHTO Category E to that consistent with an AASHTO Category B. However, it should be noted that if the same statistical approach

used to derive the AASHTO fatigue design curves is followed, the high variance of the results would lead to a much more modest increase in fatigue category.

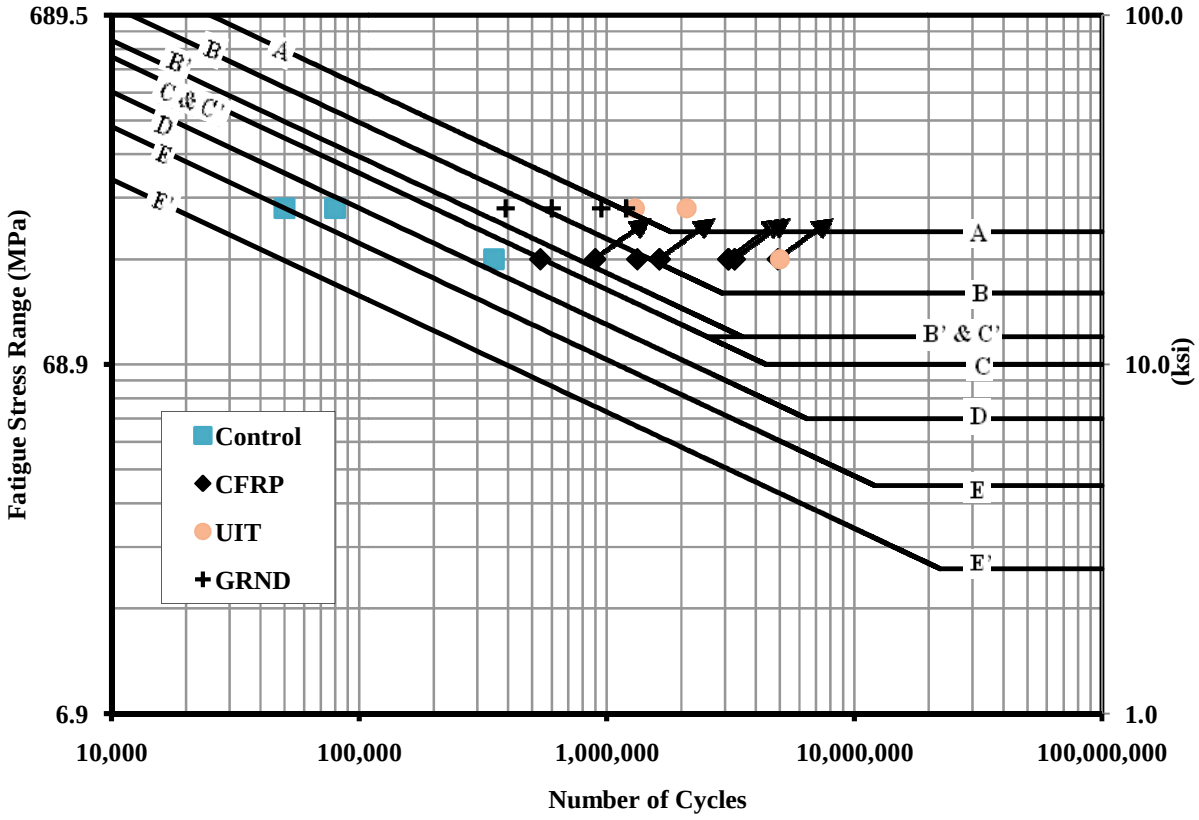

Figure 13 : Fatigue Life of Welded Connections for Various Types of Treatments

Figure 13 shows that treating the specimens with composite overlays or treating the weld with Ultrasonic Impact Treatment were equally effective, extending fatigue life to run-out in both instances.

Fatigue-Crack Propagation Life of the Welded Connections with CFRP Overlays

One of the specimens, designated TRI 04, was previously tested by Kaan (2008) and developed a fatigue crack after 1.36M cycles. This specimen was repaired with CFRP overlays with breather cloth embedded in the resin layer. The fatigue crack, detected using dye penetrant after testing by Kaan (2008), was approximately 1.6 mm (0.0625 in.) long. This pre-cracked specimen was reinforced with CFRP overlays with a 6.4 mm (0.25 in.) thick resin layer, and subjected to additional fatigue loading. After 1.3M cycles into the additional testing, the CFRP overlays were removed to inspect for fatigue cracks. After inspection, the overlays were reattached and the specimen loaded until a total of 2.88M cycles were reached. The final inspection showed that the crack length had not changed significantly.

It is meaningful to compare experimental results to theoretical fatigue life predictions. Theoretical calculations of fatigue-crack propagation life were performed using two different underlying assumptions: (1) a surface crack in an infinite plate, and (2) an edge crack in a finite plate. The theoretical model based on the assumption of an edge crack in a finite plate (Cartwright et al. 1976) captured the known thickness and known width of the steel specimen. It assumed a semi-elliptical edge crack subjected to uniaxial tensile stress. These theoretical predictions were compared with experimental measurements of crack length at a known number of fatigue cycles after crack initiation, as presented in Fig. 14. This theoretical calculation, based on the assumption of an edge crack in a finite plate, yielded the closest match to experimental results obtained by Vilhauer (2007) using a control specimen. The experimental results obtained by Vilhauer, taken from a specimen subjected to a stress range of 193 MPa (28.0 ksi), are shown for reference in Fig. 14. Other theoretical models that were considered (e.g. surface crack in a

finite plate) produced results that lay between those of the surface crack in an infinite plate and the edge crack in a finite plate. Therefore, for clarity, only the former and latter theoretical crack growth predictions are presented in Fig. 14.

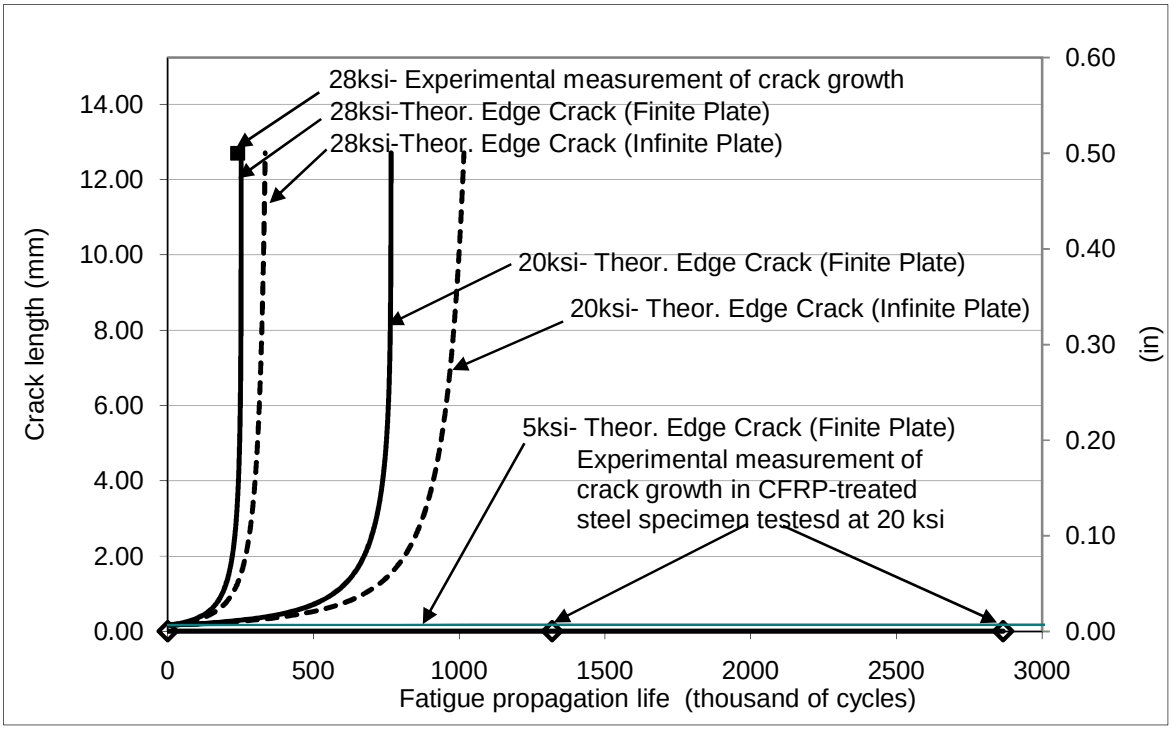

Figure 14 : Theoretical and experimental propagation life of untreated and CFRP retrofitted three-point bending specimens

Theoretical crack propagation rates were examined at various stress ranges, with the aim of determining the actual stress range the welded connection was subjected to when CFRP overlays were bonded to the specimens. It was found that the experimental crack lengths measured in steel specimens retrofitted with CFRP overlays (shown in Fig. 14 as diamond symbols) were in close agreement with the theoretical crack growth estimates for bare steel specimen subjected to a 34.5 MPa (5.0 ksi) stress range. Therefore, this exercise suggests that a

Category E' specimen with CFRP overlays bonded to it and tested at a stress range of 138 MPa (20.0 ksi) may be expected to perform similarly to an identical bare steel specimen tested at a stress range of 34.5 MPa (5.0 ksi), suggesting a reduction of 80% in the stress demand, which is consistent with results from the Finite Element Analyses.

Pullout Test Results

As previously discussed, fatigue tests showed a significant improvement in bond under fatigue loading when breather cloth was embedded in the resin layer. Tests to evaluate the bond strength between the composite and the steel showed that the use of breather cloth had a significant effect on bond strength under monotonic loading. Specimens with a 6.4 mm (0.25 in.) thick bond layer sustained a failure load 26% higher when breather cloth was embedded in the bond layer than specimens without breather cloth. In specimens with a 3.2 mm (0.13 in.) thick resin layer, the increase in failure load caused by the breather cloth was 17%. For specimens with a 1.6 mm (0.063 in.) thick resin layer, the magnitude of the failure load was not sensitive to the presence of breather cloth. It is likely that the low ratio of resin volume to breather cloth volume in the 1.6 mm (0.063 in.) thick resin layer was the reason for lack of any effect. The breather cloth fabric was 2.4 mm (0.094 in.) thick, and when embedded in a 1.6 mm (0.063 in.) thick resin layer it had to be compressed to reach the target thickness, resulting in a significantly lower ratio of resin to breather cloth volume. A low ratio of resin to breather cloth volume may have caused a weaker bond between the CFRP and steel because the resin has a significantly higher strength than the breather cloth fibers. Although the average peel stress observed for the 1.6 mm (0.063 in.) thick resin specimens was insensitive to presence of breather cloth, the observed failure mode was affected by the embedment of breather cloth. In specimens without

breather cloth, the mode of failure was more brittle than observed in tests with breather cloth (Fig. 15), with the latter exhibiting a larger deformation at failure and a residual strength on the order of 30%, both of which are indicative of greater toughness**.**

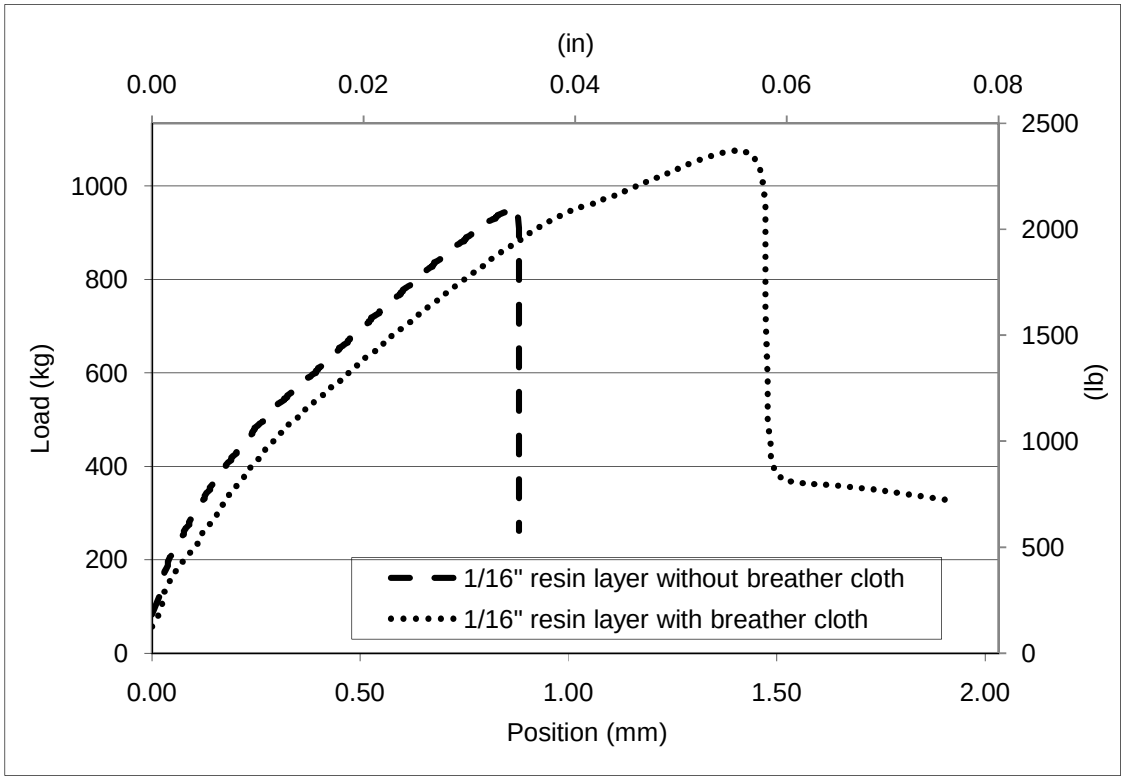

Figure 15 : Pull-out test results of 1.6 mm (0.063 in.) thick resin layer with and without breather cloth.

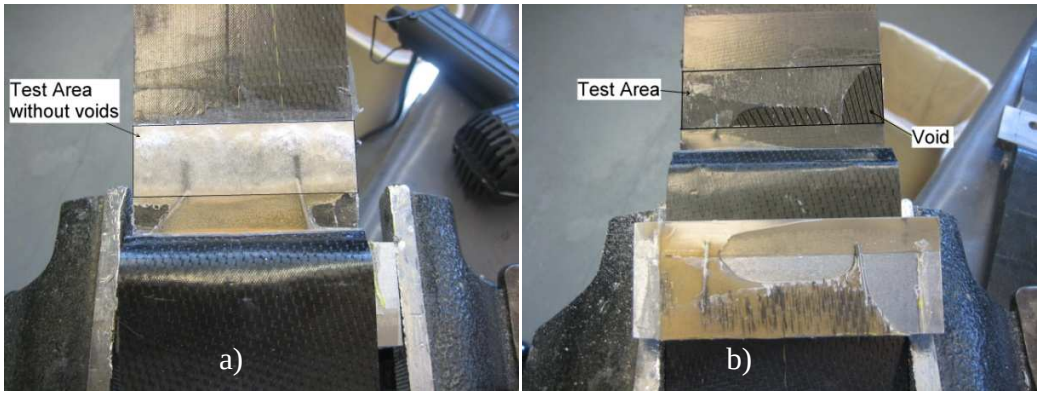

Figure 16 : Comparison of voids in bond layer (a) with breather cloth and (b) without breather cloth.

It is evident from the pullout and fatigue tests that the use of breather cloth addressed two different problems related to the bond of the CFRP overlays. The first was to eliminate as much as possible the presence of voids in the resin that tend to form during the mixing process. The use of a layer of breather cloth allowed the air bubbles in the resin to escape, significantly reducing the voids left in the bond layer after curing (Fig. 16). The second effect of adding the breather cloth was to prevent the propagation of fatigue cracks through the interface resin layer under fatigue loading.

Conclusions

There are several techniques that may be used to increase the fatigue crack initiation life in welded connections. Options for reducing crack growth rate in welded connections are much more limited, due to difficulties presented by complex geometry that often exists at fatigue details. This study focused on the use of CFRP overlays to repair and strengthen welded connections of structural steel members. It was found that using CFRP overlays was highly

effective both as a preventive measure to extend the crack-initiation life of welded connections and as a repair measure to reduce the stress demand in welded connections below the crack propagation threshold. An improvement in fatigue crack initiation life of at least 10.5 times was recorded for specimen TRI 06, and at least 10 times for specimen TRI 07, when compared with the fatigue-crack initiation life of untreated steel specimens. Composite overlays were as effective as other established repair methods such as UIT (ultrasonic impact treatment), which have been shown to provide significant improvements in fatigue-crack initiation life (14x, reported in Vilhauer (2007)).

The CFRP-retrofitted pre-cracked specimen sustained an additional total of 2.88M cycles after crack initiation without any measurable crack growth. This test showed that the CFRP overlays were able to reduce the stress range at the critical point of the welded connection below the crack propagation threshold.

Given the relatively simple bonding techniques employed, it is anticipated that with the proper level of training, this repair technique will be equally effective under field conditions, although it is recognized that there are some important considerations to be addressed before it is practical to do so with confidence.

A study of CFRP overlays to strength welded connections under fatigue loading that with impaired loading technique, the fatigue strength of welded connections can be impaired significantly.

Reference:

AASHTO, L. 2004. Bridge Design Specifications (2004). *American Association of State Highway and Transportation Officials*.

Albrecht, P., and A. Lenwari. 2007. Fatigue-proofing cover plates. *Journal of Bridge Engineering* 12 (3):275-283.

ASTM, D. 2000. 3039/D 3039M,". *Standard Test Method for Tensile Properties of Polymer Matrix Composite Materials*.

Barsom, JM, and ST Rolfe. 1999. *Fracture and fatigue control in structures: applications of fracture mechanics*. Vol. 3rd: ASTM International.

Cartwright, DJ, and DP Rooke. 1976. The compounding method applied to cracks in stiffened sheets. *Engineering Fracture Mechanics* 8:567-563.

Kaan, B, R Barrett, C Bennett, A Matamoros, and S Rolfe. 2008. Fatigue Enhancement of Welded Coverplates Using Carbon Fiber Composites.

Nakamura, H., W. Jiang, H. Suzuki, K. Maeda, and T. Irube. 2009. Experimental study on repair of fatigue cracks at welded web gusset joint using CFRP strips. *Thin-Walled Structures* 47 (10):1059-1068.

Petri, B. 2008. Finite element analysis of steel welded coverplate including composite doublers, University of Kansas.

Sabelkin, V., S. Mall, M. A. Hansen, R. M. Vandawaker, and M. Derris. 2007. Investigation into cracked aluminum plate repaired with bonded composite patch. *Composite Structures* 79 (1):55-66.

Schubbe, J. J., and S. Mall. 1999. Investigation of a cracked thick aluminum panel repaired with a bonded composite patch. *Engineering Fracture Mechanics* 63 (3):305-323.

Tavakkolizadeh, M, and H Saadatmanesh. 2003. Fatigue strength of steel girders strengthened with carbon fiber reinforced polymer patch. *Journal of Structural Engineering* 129 (2):186-196.

Vilhauer, B. 2007. Fatigue behavior of welded connections enhanced with UIT and bolting, University of Kansas.

Acknowledgment

The authors are grateful for support from the Kansas Department of Transportation (KDOT) and the University of Kansas Transportation Research Institute (KU TRI). The authors would also like to appreciatively acknowledge support provided through Pooled Fund Study TPF-5(189), which includes the following participating State DOTs: Kansas, California, Iowa, Illinois, New Jersey, New York, Oregon, Pennsylvania, Tennessee Wisconsin, and Wyoming, as well as the Federal Highway Administration.

IMPROVED METHOD FOR BONDING CFRP OVERLAYS TO STEEL FOR FATIGUE REPAIR

Abstract

Experiments and computer simulations were carried out at the University of Kansas to investigate the use of composite materials for strengthening and repair of fatigue-vulnerable steel bridges. Prefabricated CFRP overlays were attached to welded coverplate specimens using a layer of epoxy resin. The specimens were then subjected to three-point bending under cyclic loading at a constant stress range. Early tests showed that bonding CFRP overlays to steel was an effective method to reduce the stress demand in areas susceptible to fatigue damage, and that this strengthening method could lead to substantial increases in crack initiation life. Fatigue tests also showed that maintaining the bond between the CFRP overlays and the steel was the most critical factor in the effectiveness of this strengthening technique. It was observed that the presence of a layer of breather fabric embedded within the layer of epoxy resin was the most important parameter affecting bond behavior under fatigue loading.

This paper describes monotonic and fatigue tests carried out to evaluate the effect of the presence of breather fabric and thickness of the resin layer on bond strength and on the performance of the resin layer under fatigue loading. It was found that the mode of failure of the resin under monotonic and fatigue loading changed significantly due to the presence of the breather cloth. Although the presence of breather cloth had a negligible effect on the bond strength of thin resin layers, its effect on strength increased with the thickness of the resin layer. It was also found that the presence of the breather fabric had a very significant effect on the post-

peak behavior of monotonic tests, which partially explains its beneficial effect on behavior under fatigue loading.

Background

Techniques to strengthen connections vulnerable to fatigue damage in steel bridges must be developed taking into account the specific characteristics of each particular detail. However, there are some common principles that can be used as a guide to develop new solutions. Several studies conducted at the University of Kansas have investigated the concept of using composite

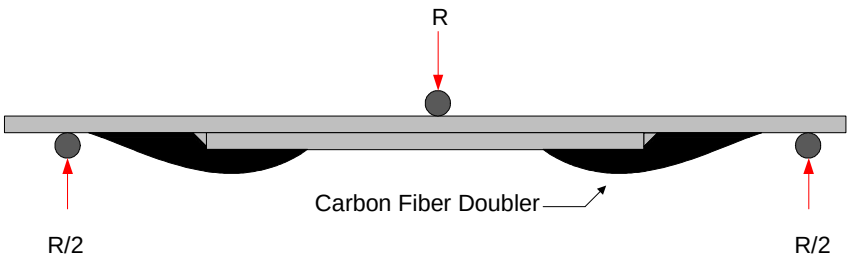

Figure 1: Fatigue Specimen Strengthened with Composite Overlays

materials to strengthen fatigue-vulnerable connections in steel bridge structures. An example of the type of specimen used at Kansas to evaluate this strengthening technique is shown in Fig. 1. The specimen consists of two plates welded together and subjected to three point bending under fatigue loading. This specimen was chosen because a severe discontinuity exists at the point where the two plates are welded, and the stress concentrations in the discontinuity lead to fatigue failure under cyclic loading.

Computer simulations of the specimen shown in Fig. 1 performed for this study using the Finite Element Analysis program ABAQUS showed that attaching overlays made with composite materials to areas of the specimen affected by stress concentrations (areas adjacent to

the welds) led to significant reductions in the localized stress demand. This effect is shown in Fig. 2 which shows the maximum stress demand at the weld region of the specimen for configurations with and without a composite overlay. The Finite Element results indicated that the composite overlays were effective in providing an alternate load path to the force transmitted between the two steel plates, spreading the stress demands over a larger area and consequently reducing the stress gradient.

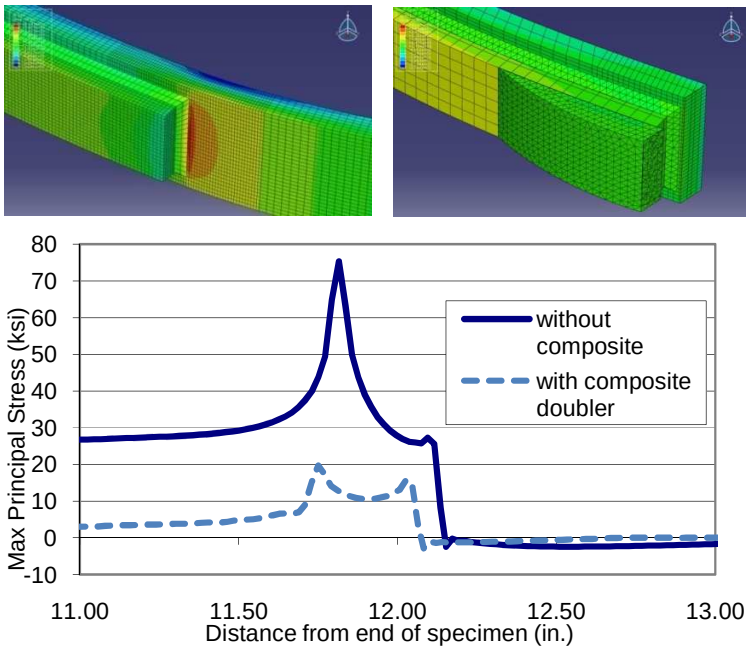

Figure 2 Maximum Principal Tensile Stress for (a) unreinforced specimen, (b)

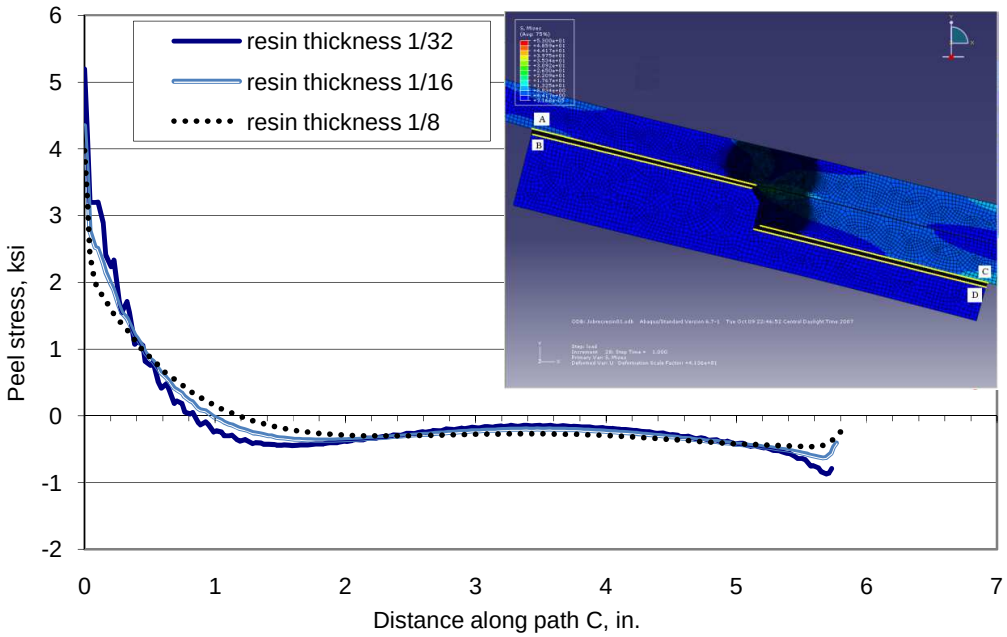

Figure 3: Peel stress demand along path C for various thicknesses of epoxy resin

One of the most significant challenges associated with the implementation of this retrofit technique is developing a fabrication process that results in stiff overlays that are properly bonded to steel elements. Although composite plies can be applied directly on the field, better results are obtained by prefabricating the overlays in shop and subsequently attaching them to a bridge. However, this fabrication sequence brings about challenges, for example, because the composite overlay may not align perfectly with the steel, and because a method of properly bonding the overlay to the steel must be developed. In this study, composite overlays were prefabricated following the procedure described by Kaan (2008) and attached to three-point bending specimens shown in Fig. 1 by means of a layer of epoxy resin between the composite overlay and the steel. Finite element models were developed to investigate the effect of varying the thickness of the layer of epoxy resin on the stress demand at the toe of the weld, and on the shear and tensile stresses at the interface between the resin layer and the steel (Petri, 2008).

Calculated stress demands using the Finite Element model are shown in Fig. 3. In the case of the three-point bending specimen the thickness of the resin layer had a significant effect on the peel stress between the epoxy resin and the steel. A similar effect was observed for the peel stress between the epoxy resin and the composite overlay. The magnitude of the maximum peel stress was significantly different on each side of the epoxy resin layer and it was found to increase with decreasing thickness of the epoxy resin layer.

Kaan (2008) and Alemdar performed tests to evaluate experimentally the results from the Finite Element study. Their results are illustrated in Fig. 4.

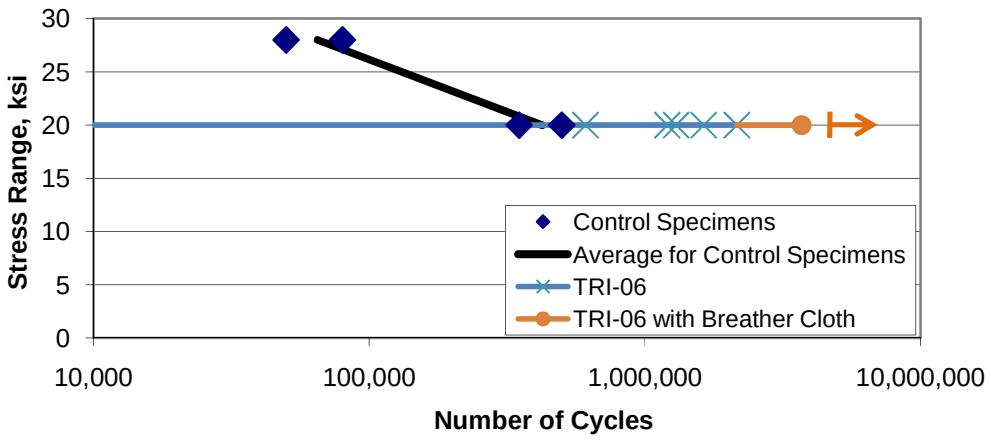

Figure 4: Crack Initiation Life for Three-point Bending Specimens Tested by Kaan and Alemdar.

The diamond shapes in Fig. 4 represent the initiation life of 4 control specimens tested at nominal stress ranges at the weld toe of 20 and 28 ksi (Kaan, 2008). The average initiation life of the control specimens tested at a nominal stress range of 20 ksi was 425,000 cycles. The points

labeled TRI 6 correspond to multiple fatigue tests performed by Kaan (2008) and later by Alemdar as part of this study using a single three-point bending specimen strengthened with composite overlays, at a nominal stress range of 20 ksi. Kaan (2008) performed his tests with a layer of epoxy resin 1/16th of an in. thick. The X-shaped markers correspond to points at which Kaan (2008) observed debonding of the composite overlay. Each time after debonding was observed, the specimen was inspected and the overlay re-attached. Kaan (2008) loaded the specimen for a total of 2.1 million cycles without any observable fatigue crack. There were a total of 5 debonding events, with an average of 431,500 cycles between debonding events. Loading of the specimen was later continued by Alemdar (shown by the round markers in Fig. 4). He used a ¼-in. thick epoxy resin layer with embedded breather cloth. Alemdar was able to load the specimen for an additional 1.5 million cycles without any debonding events. After loading for 1.5 million additional cycles (for a total of 3.7 million cycles) the overlay was removed and an inspection showed that there were no observable fatigue cracks.

The tests performed by Alemdar and Kaan showed that the use of composite overlays increased the initiation life of the specimen from 425,000 cycles to infinite fatigue life, confirming the observations from the Finite Element Analyses. The aforementioned tests also showed that the presence of breather cloth increased the fatigue life of the epoxy resin layer from an average of 431,000 cycles to infinite fatigue life. Proper bond is critical to the performance of this strengthening method because if an overlay debonds the specimen continues to cycle in the unreinforced configuration until a repair is implemented. For this reason, and because the observed fatigue life of specimens with breather cloth was significantly higher than those without breather cloth, a series of experiments was undertaken to study the effects of embedding breather cloth on the bond strength and fatigue life of the epoxy resin layer.

Experimental Study

The effects of embedding breather cloth on the strength and fatigue life of the epoxy resin layer were further studied by performing two series of monotonic tests. The monotonic tests were designed to simulate the state of stress in the epoxy resin layer of three-point bending specimens. For the first series of tests a composite overlay similar to those used to strengthen the plate-coverplate specimen was attached through a steel plate using a layer of epoxy. The test apparatus and its dimensions are shown in Fig. 5.

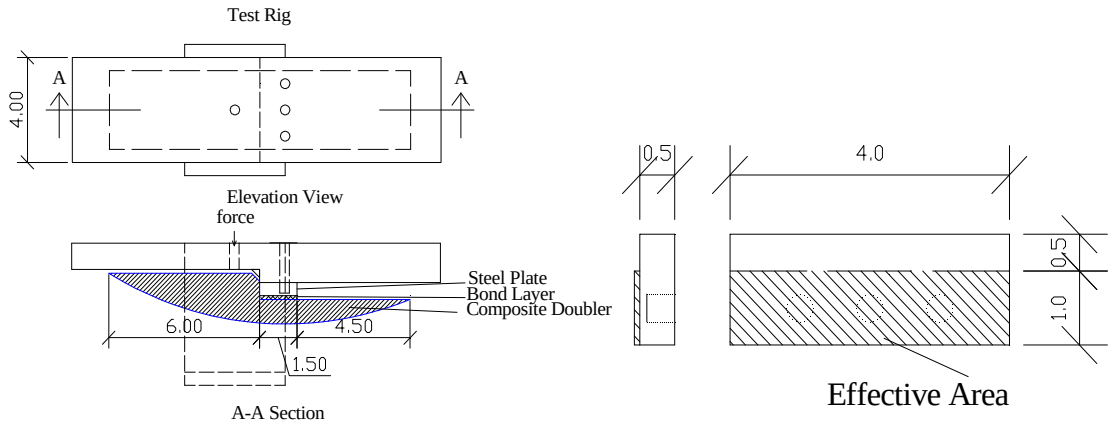

Figure 5 : Test Apparatus for Peel Tests (all dimensions in in.

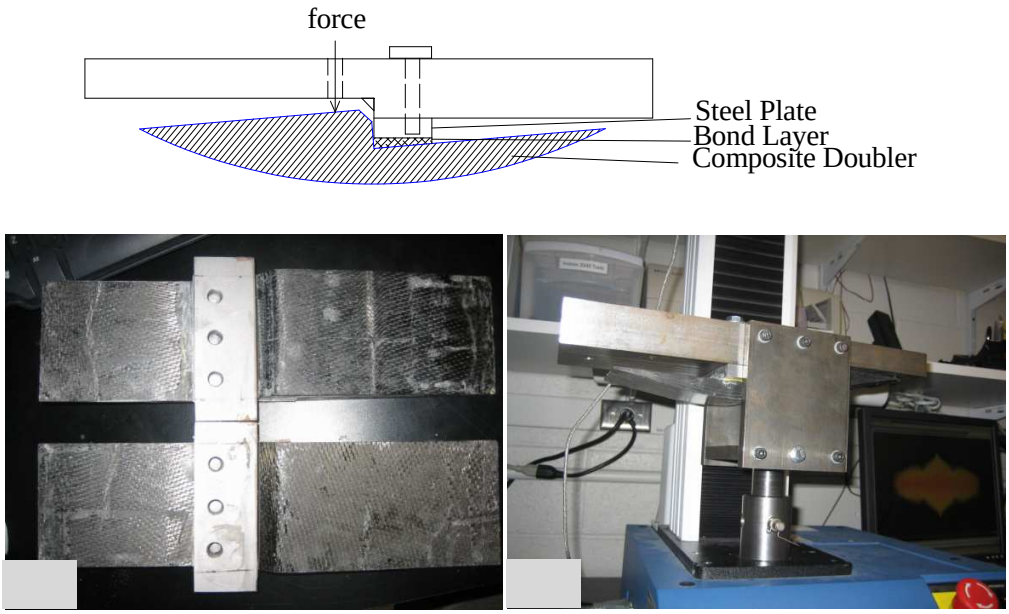

Figure 6: Composite Overlays Attached to Steel Plate: (a) Diagram of Loading Apparatus, (b) Steel Plates Bonded to Composite Overlays, (c) Reaction Apparatus Installed in Testing Machine.

Monotonic tests were performed according to the following protocol. The composite overlay was bonded to the steel plate with a layer of epoxy of a pre-determined thickness. The steel plate was subsequently bolted to the reaction apparatus, which was attached to the testing machine. The specimen was loaded using a pin that was pushed through a hole in the plate (Fig. 6), inducing a state of stress in the resin layer that combined the effects of direct tension and bending (Fig 7). The part of the plate opposite the loading pin was machined to avoid direct contact between the composite and the reaction plate (Fig. 6).

Finite Element analyses were performed to compare the state of stress in the resin layer of the monotonic tests and the resin layer of the three-point bending specimen. Results from the finite element analysis are shown in Fig. 7. Although the stresses shown in Fig. 7 do not

constitute a perfect match of those in Fig. 3, important features are repeated. In both cases the normal stresses vary following a gradient from tension to compression, indicative of combined tension and bending, with peak values at the edge of the resin layer.

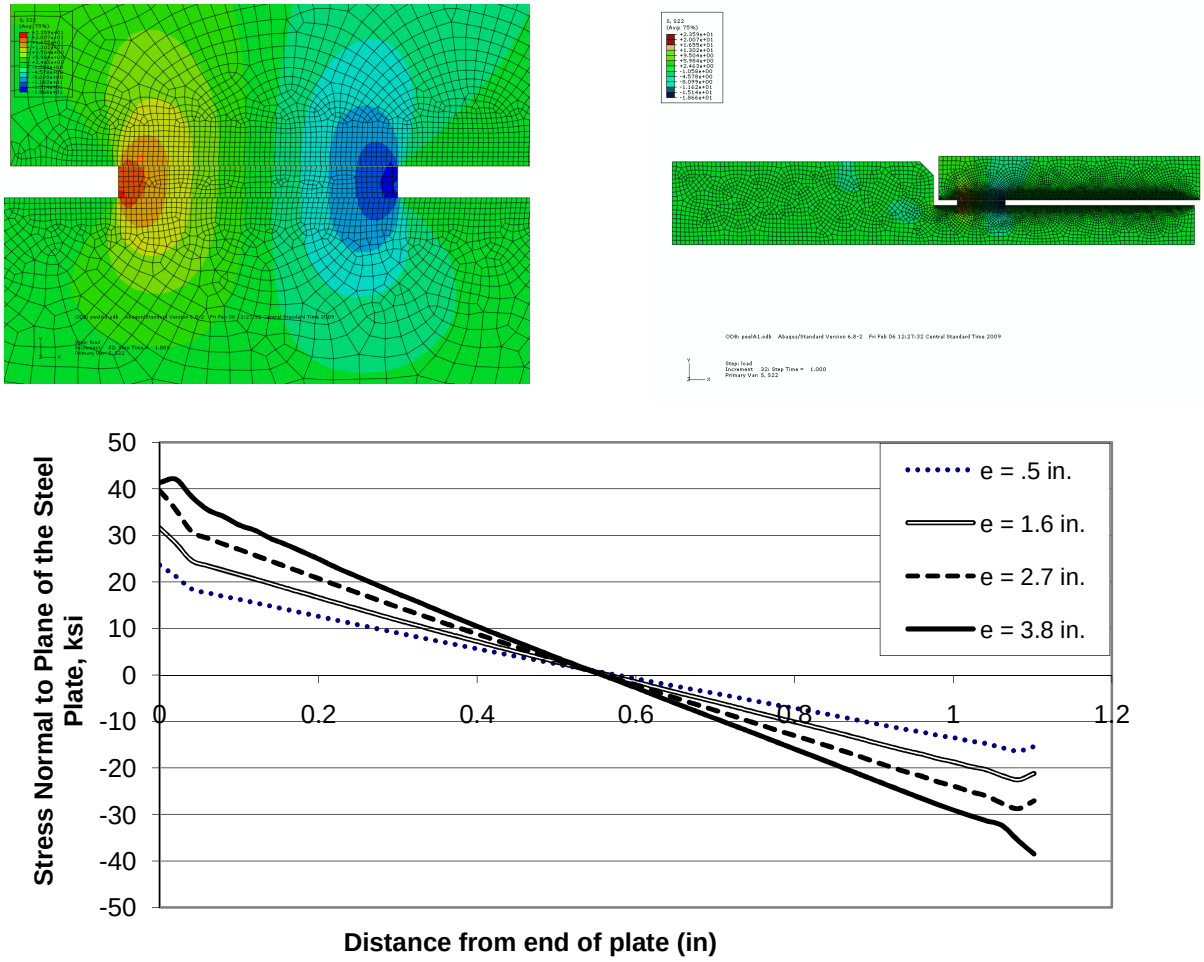

Figure 7:. Stress Demand on the Resin Layer (a) Finite Element Fringe Showing Stresses Normal to the Plane of the Plate, (b) Finite Element Mesh, (c) Calculated Tensile (Peel) Stress at the Steel-Resin Interface for Various Pin Eccentricities (in units of in.)

Results

For the first series of monotonic tests, in which the resin layer was used to bond a steel plate to the composite overlay, most failures were due to delamination within the composite overlay instead of loss of bond between the resin layer and the steel (Fig. 8). This was likely due to the fact that the resin used to bond the composite to the steel (Hysol) was stronger than the resin used to fabricate the composite overlay. Measured load-deflection relationships for the specimens tested are shown in Fig. 8. The dashed lines in Fig. 8 correspond to resin layers with embedded breather cloth, while the solid lines correspond to specimens without breather cloth. As shown in Fig. 8 the average peel stress ranged between 100 and 300 psi.

The failure of one of the specimens without breather cloth illustrates one of the most important effects of embedding breather cloth within the resin layer. Due to the low viscosity of the resin, large voids formed in the resin layer during fabrication, resulting in much weaker bond between the resin layer and the steel. This was the only instance in which failure occurred due to loss of bond between the resin layer and the steel instead of debonding of the composite.

Because the main objective of the study was to evaluate the bond between the resin layer and the steel the test was modified to avoid premature failure due to delamination of the composite. For a second series of tests the composite overlay was replaced by a steel plate, guaranteeing that failure would be caused by loss of bond between the epoxy and the steel.

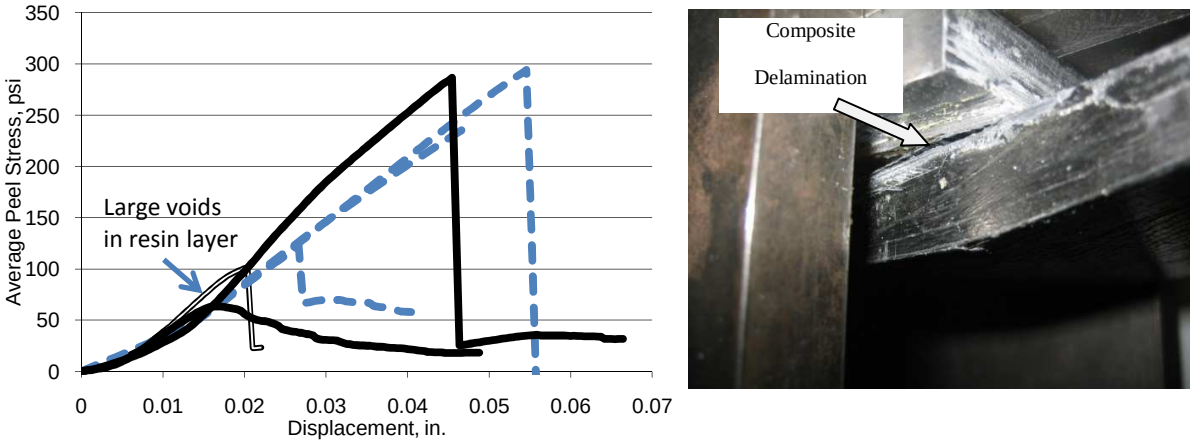

Figure 8: Monotonic Peel Tests of Epoxy Resin Layer with Composite Overlays.

The steel plate used to replace the composite overlay had dimensions of 1-½ in. wide, 4 in. long, and ½-in. thick. Of the steel plate, only a 1-in. wide strip was bonded to the resin. The remaining ½-in. was covered with Teflon tape to prevent bond with the steel (Fig. 5). In the same manner as the first group of tests, there were specimens with and without breather cloth embedded in the epoxy resin layer.

The specimens were prepared according to the following procedure. The surface of the two plates was roughened with a grinder and subsequently cleaned with acetone and methanol. The edge of the area to be bonded was covered with adhesive tape in order to build a dam for the resin. In specimens with embedded breather cloth the cloth was cut leaving a hole to allow placing of a spacer to maintain the thickness of the resin. At this point the resin was prepared by mixing and poured in the bond area. When cloth was used, it was verified that the cloth absorbed the resin evenly, and that sufficient resin was absorbed by the cloth. The second steel plate was then placed on top of the resin pool making sure that the plate was in contact with the spacer. Pressure was maintained with a clamp throughout the curing process.

A total of 14 peel tests were performed to evaluate the effect of resin layer thickness and presence of breather cloth on the average tensile stress at failure. Resin layers tested had thicknesses of 1/16 in., 1/8 in., and ¼ in. Specimen characteristics and the average peel stress at failure are summarized in Table 1. The average peel stress was calculated as the maximum measured force divided by the effective bond area. This simple quantity was considered an adequate to establish a basis of comparison between the different configurations.

Load-displacement curves for the peel tests are shown in Fig. 9. Curves with dashed lines correspond to specimens with cloth, while solid lines correspond to load-deformation curves for specimens without cloth. In general, specimens with breather cloth achieved significantly higher deformations at failure. Another trend that was observed was that in specimens without breather cloth failure was sudden and led to a total loss in bond between the two plates. Specimens with breather cloth retained a residual capacity of approximately 30% of the maximum stress.

Figure 10 shows the resin layer of specimens with and without breather cloth after failure. Figure 10 shows that while the resin layer without cloth developed voids (Fig. 10 a), the resin layer with breather cloth did not. Furthermore, it was observed that in the resin layer with breather cloth failure occurred through the middle of the resin layer, with residues remaining attached to both steel plates. This is an indication that the tensile strength of the resin was the limiting factor, and not the bond strength between the steel and the resin. Figure 11 shows the appearance of the steel plates after failure for specimens with a resin layer thickness of 1/8-in. and ¼-in. Another feature that was observed was that in specimens with thinner resin layers failure tended to occur through the middle of the resin layer, while in specimens with thicker resin layers the tendency was for a larger amount of resin remaining attached to one of the two plates.

Table 1: Results from Peel Tests of Steel Plates

Specimen Designation	Thickness (in.)	Cloth (y/n)	Average Peel Stress (psi)
1	0.0625	n	737.4
2	0.0625	n	601.4
3	0.0625	y	644.9
4	0.0625	y	677.4
5	0.1250	n	501.1
6	0.1250	n	360.6
7	0.1250	n	512.9
8	0.1250	y	488.3
9	0.1250	y	584.6
10	0.1250	y	535.4
11	0.2500	n	274.6
12	0.2500	n	371.1
13	0.2500	y	381.7
14	0.2500	y	434.3

Figure 10 shows the relationship between the tensile (peel) strength of the resin layer and the thickness of the resin layer for specimens with and without breather cloth. Figure 10 shows that the strength of the resin layer decreased with increasing thickness, and that the reduction in strength with thickness was less pronounced for specimens with breather cloth. Also, it was observed that for specimens with very thin resin layers the presence of breather cloth had a negligible effect on strength, while for layers 1/4 –in. thick the difference in strength was on the order of 25%. These results suggest that using a resin layer with a thickness of at least 1/8 in. with embedded breather cloth will provide the best results. The observed benefits of breather cloth were a lower propensity to develop voids in the resin layer, higher strength (for layers with a thickness of at least 1/8 in.), and a significant residual strength after cracking, which is likely to slow crack growth under fatigue loading.

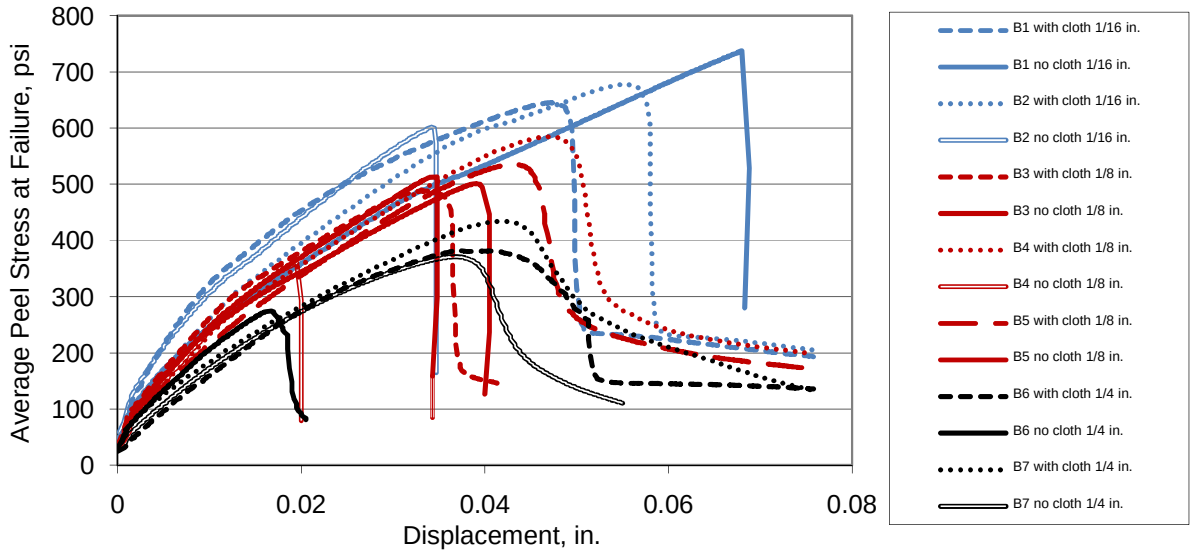

Figure 9: Monotonic Peel Tests of Epoxy Resin Layer with Steel Plates.

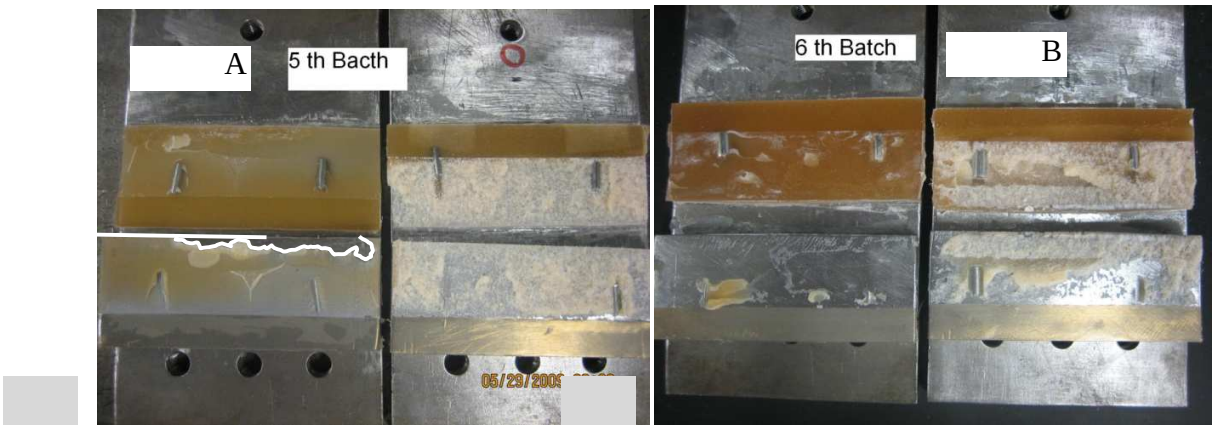

Figure 10: Appearance of Resin Layer after Failure for Specimens from (a) Batch 5 (1/8-in. thick) and (b) Batch 6 (1/4-in. thick).

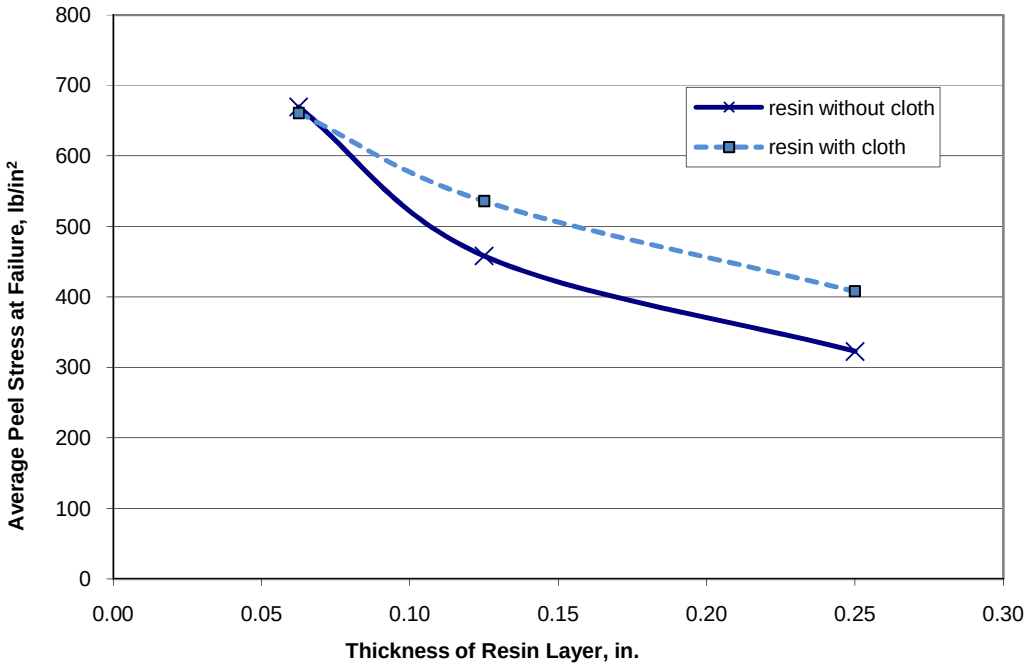

Figure 11: Effect of Resin Layer Thickness on Peel Strength of Epoxy Resin Layer

Conclusions

Monotonic tests were performed to develop a better understanding of the effects of the thickness of the resin layer and the presence of breather cloth on the fatigue life of the epoxy resin layer. It was found that the use of breather cloth eliminated the occurrence of large voids in the resin layer, which can act as a trigger for fatigue cracks and significantly reduce the fatigue performance of the bond layer. Although thicker layers resulted in lower peel strength, these were less susceptible to problems with voids. Another benefit associated with the use of breather cloth was in terms of ductility. The monotonic tests showed that after failure of the resin took place, the breather cloth was capable of tying together the two sides of the failure surface,

resulting in a residual capacity of approximately 30% of the strength of the resin. In terms of fatigue behavior, this type of post-peak behavior shows that breather cloth likely has the effect of retarding the growth of fatigue cracks within the bond region. Both of these effects result in a significant improvement in the bond strength under fatigue loading between composite overlays and steel elements, which is consistent with the improvements in behavior observed in fatigue tests of three-point bending specimens.

Computer simulations and fatigue tests performed as part of this study showed that composite overlays were capable of significantly extending the fatigue life of steel structures as long as adequate bond was maintained between the overlays and the steel. Fatigue tests also showed that excellent performance for this type of repair could be achieved by prefabricating composite overlays and attaching them to the steel structures using a layer of epoxy resin with embedded breather cloth.

References

Kaan, B. (2008). "Fatigue Enhancement of Category E' Details in Steel Bridge Girders using CFRP Materials," MS Thesis, University of Kansas at Lawrence.

Petri, B. (2008). “Finite Element Analysis of Steel Welded Coverplate Including Composite Doublers,” MS Thesis, University of Kansas, Lawrence.

Acknowledgment

The authors are grateful for support from the Kansas Department of Transportation (KDOT) and the University of Kansas Transportation Research Institute (KU TRI). The authors would also like to appreciatively acknowledge support provided through Pooled Fund Study

TPF-5(189), which includes the following participating State DOTs: Kansas, California, Iowa, Illinois, New Jersey, New York, Oregon, Pennsylvania, Tennessee Wisconsin, and Wyoming, as well as the Federal Highway Administration.

USE OF CFRP FOR REPAIR OF FATIGUE CRACKS IN STEEL PLATE UNDER TENSION LOADING

Abstract

A total of five specimens with pre-existing fatigue cracks were tested under cyclic loading to evaluate the performance of composite overlays to repair fatigue damage in steel structures. Two were control specimen with no overlay. The other three of the specimens were repaired with Carbon Fiber Reinforced Polymer (CFRP) overlays. Two of the specimens were repaired using multi-layered overlays prefabricated with CFRP plies. The overlays in the third specimen were fabricated using a spray fiber system. The composite overlays were removed for inspection and re-attached every million cycles to track fatigue-crack propagation. It was found that specimens repaired with composite overlays had fatigue crack propagation lives each exceeding 3 million cycles, while the observed propagation life of untreated specimens was below 60,000 cycles. Results from a series of Finite Element Analyses showed that the peak stress demand was reduced by approximately 80% with the addition of composite overlays when compared to untreated specimens, which is consistent with the observed change in fatigue-crack propagation life in the experiments.

Introduction and Background

A significant number of aging steel bridge structures experience structural problems due to fatigue cracks. After fatigue cracks become large enough to be detected, some repair measure must be undertaken to prevent structural failure of the member and potentially serious damage to the bridge. Methods that have been used in the past to repair fatigue cracks in metal structures

include welding, ultrasonic impact treatment, bolting, and the attachment of fiber reinforced polymer (FRP) overlays. FRP overlays may be used as a preventive measure to enhance the fatigue life of a bridge or as a repair method to arrest cracks and prevent further crack growth.

This study investigates the use of carbon fiber reinforced polymer (CFRP) overlays to repair fatigue cracks that have already been detected. The main advantage of CFRP overlays is that, if proportioned and bonded properly to the steel, the stress field in a vulnerable element or connection can be reduced significantly, reducing the stress demand and increasing fatigue life. One of the most important concerns when implementing this repair method is to achieve adequate bond between the steel and the composite overlay. Voids or imperfections in the layer of resin that is used to attach the composite overlay to the underlying metal can lead to the formation and propagation of fatigue cracks within the resin. Preventing the initiation of fatigue cracks within the bond layer is of paramount importance because these cracks can eventually cause debonding of the overlay, rendering the repair ineffective.

A significant amount of research on the use of composite materials to repair fatigue cracks has been carried out in the field of aerospace engineering to address fatigue problems in the fuselages of airplanes (Mall et al. 2009; Umamaheswar et al. 1999; Schubbe et al. 1999; Naboulsi et al. 1996; Lee et al. 2004; Liu, Xiao et al. 2009). Consequently, most research performed on this topic in the aerospace field has focused on use of FRP patches to repair fatigue damage in aluminum plates.

Bonding of CFRP patches to aluminum panels in the aforementioned studies is an elaborate process. For example, in an experimental study performed by Sabelkin et al, (2006), a grit blast/silane (GBS) surface preparation technique was used that involved grit blasting the

aluminum surface, applying a hydrolyzed silane solution that was cured at 104 °C (219 °F) for one hr. after being applied, and later sprayed with a corrosion inhibiting primer.

In general, researchers in the aerospace field classify aluminum plates in terms of thickness, with a thickness of 6.0 mm (0.24 in.) considered to be the threshold between thin and thick plates (Sabelkin et al. 2006). A commonly used parameter for proportioning composite patches for the purpose of repairing fatigue damage is the ratio of axial stiffness of the composite patch to the axial stiffness of the plate (Sabelkin et al. 2006). The ratio is defined as:

$$SF = E_{FRP}\, t_{FRP} / E_s\, t_s \qquad (1)$$

where SF is the stiffness ratio, E_{FRP} is the modulus of elasticity of the FRP, t_{FRP} is the thickness of the FRP patch, E_s is the modulus of the steel, and t_s is the thickness of the steel plate. The SF parameter is used to determine the number of layers needed to repair fatigue damaged plates by assuming that the driving force is redistributed in proportion to the relative axial stiffness of the two materials. In single-sided repairs, a stiffness ratio of 1.4 is recommended for repair of damage in thin plates and 1.0 for thick plates (Sabelkin et al. 2006).

Studies evaluating the use of FRP patches for repairing fatigue damage in the aerospace field have generated very positive results. An experimental study by Mall and Conley (2009) investigated the behavior of aluminum plates reinforced with unidirectional boron fibers. The thickness of the aluminum plate was 6.35 mm (0.25 in.) and the thickness of the fiber patch was 1.14 mm (0.045in.). The load ratio r for the specimens was 0.1, and the maximum stress was 240 MPa (38.81 ksi) in tension. Mall and Conley (2009) concluded that crack size played an important role on the fatigue-crack propagation life of specimens repaired with FRP patches, and they found good agreement between the results from Finite Element (FE) models and experimental results. The authors reported that bonding a FRP patch to only one side of the

aluminum specimen increased the fatigue-crack propagation life of the specimen between four and 10 times with respect to the fatigue life of the untreated specimen. Wang et al. (2002) also found an increase in fatigue crack propagation life, on the order of 10 times, in aluminum plates repaired with FRP patches.

Studies have been performed to investigate the use of composite overlays to repair fatigue-related damage in steel structures. (Tavakkolizadeh et al. 2003) studied the effectiveness of CFRP sheets to improve the fatigue strength of steel girders. In this study, flanges of small I-shaped steel beams (S127x4.5) were cut to create a notch crack. Unidirectional CFRP sheets were bonded over the area of the notch and the beams were tested under various stress ranges ranging from 138 MPa (20.0 ksi) to 345 MPa (50.0 ksi). Surface preparation of the steel flanges consisted of sandblasting, washing with saline solution, and rinsing. A total of six specimens were repaired with CFRP sheets and tested. Observed crack growth rates for the retrofitted beams ranged between 25% and 40% of the growth rate for unretrofitted beams. The authors reported that the fatigue-crack propagation life of the specimens with CFRP sheets was extended by a factor of approximately three compared with that of control specimens.

(Liu, Al-Mahaidi et al. 2009) studied the tensile fatigue behavior of notched steel plates strengthened with single-ply CFRP patches. One of the parameters studied was the modulus of elasticity of the carbon fiber used to manufacture the CFRP patch. One set of patches, designated high modulus, had carbon fibers with a modulus of elasticity of 640 GPa (93,000 ksi), while the other set, designated normal modulus, had carbon fibers with a modulus of elasticity of 240 GPa (35,000 ksi). Another parameter in the study was the area over which the CFRP patches were attached. Various placements were studied, including attachment over the crack,

two separate attachment areas, either covering or not covering the crack, and double or single-sided attachment of the patch (the double sided attachment consisted of bonding CFRP patches to both sides of the specimen). Specimens with double-sided patches were symmetric, which prevented the introduction of any secondary stresses associated with the CFRP repair. The authors reported that the single-sided repair extended the fatigue-crack propagation life of the specimen by a factor ranging between 2.2 and 2.7, whereas the double sided repair extended the fatigue-crack propagation life from 4.7 to 7.9. Roy et al. (2009) performed a study using the same type of materials and procedure used by Liu et al. (2009), but focused the study on the single sided repair because of the inherent asymmetry. Roy et al. (2009) paper reported an extension of fatigue-crack propagation life by a factor of 2.2 compared with that of the unrepaired case. Both Liu et al. (2009) and Roy et al. (2009) showed similar extension of fatigue-crack propagation life of steel plates repaired with single-sided CFRP patches.

Analytical modeling of CFRP repairs using the Finite Element method is also a very important tool to develop efficient retrofit schemes. To properly determine the effects of the repair through use of computer models it is important to define the materials properties of the specimen as accurately as possible. Liu et al. (2009) and Lee and Lee (2004) developed analytical models that included nonlinear material properties,and reported that such level of refinement was unnecessary if the steel plate thickness was greater than 6 mm (0.24 in.). Material nonlinearities only played an important role when the thickness of the steel plate was less than 6 mm (0.24 in.), due to the stress intensity factor.

Several researchers (Liu, Xiao et al. 2009; Lee et al. 2004) have shown good agreement between the change in stress demand predicted using FE and experimental measurements of change in fatigue crack propagation life. The aforementioned researchers defined the material

properties in their FE models as linear elastic. One of the limitations of linear elastic models is that although such models are capable of providing a good representation of the stress field, limited information can be obtained about the potential for debonding of the composite, which has been shown to be a critical mode of failure in fatigue tests. In FE models that include a layer of resin between the CFRP overlay and the underlying metal, the potential for debonding could be assessed by comparing the stress demand in the resin with a limiting value. The limiting stress, for example, could be a fraction of the shear strength of the adhesive. This approach was adopted in the FE simulations conducted in this study.

Objective and Scope

The primary objective of the study described in this paper was to investigate the use of composite materials to repair fatigue damage in steel structures. Bonding of CFRP overlays was performed using simpler techniques than those used in the aerospace field (Sabelkin et al., 2006), so that repairs would be more representative of the kind of work that can be performed under field conditions in bridge structures. Experiments were conducted to evaluate if fatigue-crack propagation under constant amplitude tensile load was similar in steel specimens repaired with two different types of composite overlays with different bonding techniques, and to evaluate if the observed performance was similar to that reported in previous studies on aluminum plates reinforced with composite patches. Additionally, a secondary objective of this research was to determine the relative effectiveness of CFRP overlays when applied to steel substrate with varied magnitude of the axial stiffness parameter, *SF*.

The study also comprised a suite of Finite Element simulations to investigate the validity of the axial stiffness parameter *SF*, frequently referenced in studies on aluminum plates, to

estimate the reduction in stress demand. The FE simulations were intended to evaluate the correlation between fatigue-crack propagation rates and computed values of Hot Spot Stress (HSS). The use of HSS as a design parameter was evaluated because it is a versatile parameter that may be used for various types of geometric configurations, materials, and loading conditions.

Computer Simulations

Computer simulations of the specimens tested during the experimental program (Fig. 1) were carried out using the commercially-available Finite Element analysis software ABAQUS version 6.8.2 (Simulia, 2009).

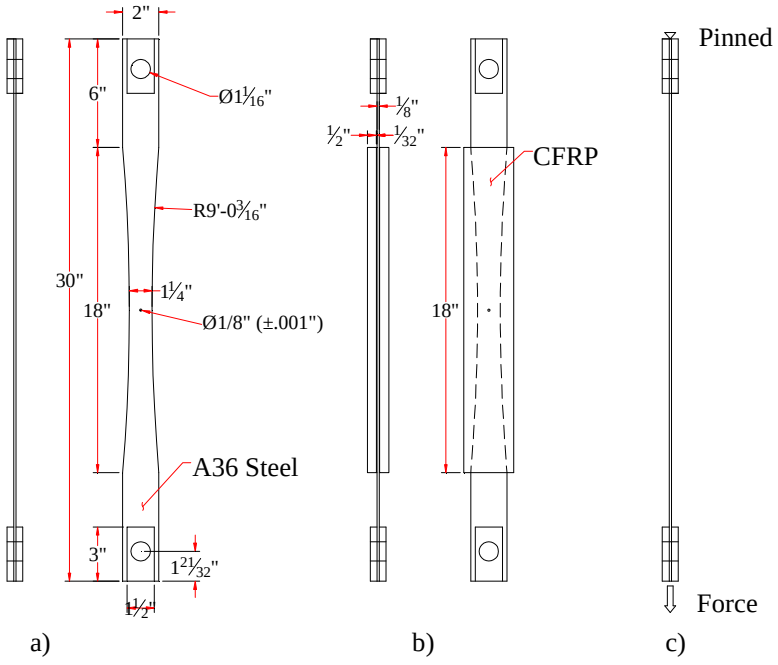

Figure 1 : Tension specimen a) bare steel b) specimen with CFRP overlay attached c) boundary and loading conditions imposed on the model

The FE models were developed using linear elastic material models and meshes were assembled using 8-node brick elements. The modulus of elasticity's for the steel, composite overlay, and resin were selected as 200, 83, and 2 GPa (29,000, 12,000, and 300 ksi), respectively. The mesh density was defined such that elements would be 0.30 mm (0.01 in.) within a region 51 mm (2.0 in.) from the center hole, and 2.5 mm (0.10 in.) in all other parts of the specimen. Interfaces between the steel and composite parts of the model were defined using tie constraints. Motion was restrained at one end of the model while the other end was free to move only in the vertical direction (Fig. 1c). Two concentrated loads were applied in the vertical direction at the unrestrained end, one on each face of the model. Maximum principal stresses, shown in Fig. 2 for a model with CFRP plates attached, were extracted along a path starting at the center of the steel plate and ending at the edge (Fig. 3) for comparison with other model results,.

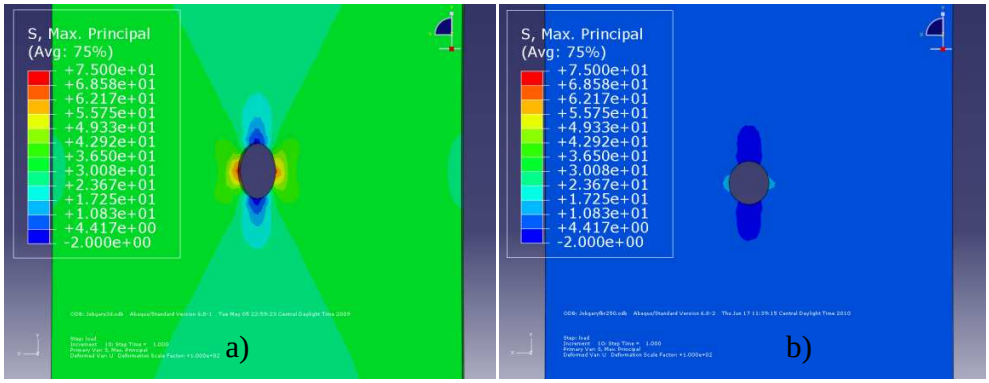

Figure 2 : Maximum principal stresses at the center of the specimen for the a) unreinforced b) reinforced condition

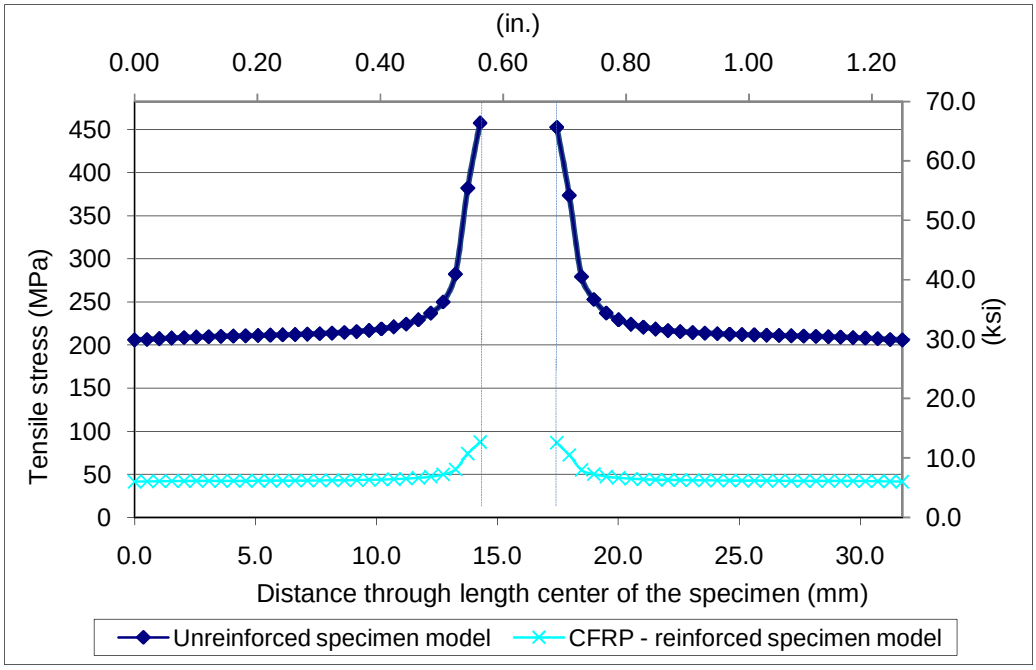

Figure 3 : Maximum principal stresses at the location of net cross-section for CFRP-reinforced and unreinforced specimens

The path was defined through points located at the mid-thickness of the steel plate, along the cross-section through the net section of the steel. The magnitude of the stress demand along the path is shown for the unreinforced and CFRP-reinforced conditions in Fig. 3. A comparison of the stresses presented in Fig. 3 indicates that reinforcing the steel specimen with composite overlays resulted in a reduction of peak stress demand by approximately 80%.

Although maximum principal stresses were extracted along the entire path through the steel net section as shown in Fig. 3, further comparisons were performed on the basis of the Hot Spot Stress (HSS). In this paper, HSS was defined as the stress at a distance half the thickness of the steel plate away from point of peak stress, which occurred at the edge of the hole in this case

(Marquis et al. 1995). Hot Spot Stress analysis was used as an indicator of stress range, and consequently, as a measure of the effectiveness of various composite overlay configurations.

The suite of computer simulations performed in this study were intended to investigate the effects of four different parameters on the fatigue performance of the retrofit scheme: modulus of elasticity of the CFRP, thickness of the CFRP overlay, length of the CFRP overlay, and thickness of the interface layer used to bond the CFRP overlay to the steel. The effects of the four parameters investigated are discussed in the following.

Effect of the Modulus of Elasticity of the CFRP

Six different models were developed to investigate the effect of the modulus of elasticity of the CFRP on stress demand imposed on the steel specimen. Each of the models discussed in this section had identical properties with the exception of the modulus of elasticity of the CFRP, which was varied between 27.0 GPa (3,860 ksi) and 138 GPa (20,000 ksi), in increments of 28 GPa (4,000 ksi). Thickness of the composite overlays was maintained as 6.4 mm (0.25 in.), length of the CFRP patch was maintained as 458 mm (18.0 in.), and the thickness of the interface layer was held at 0.600 mm (0.025 in.). The effect of CFRP modulus of elasticity on hot spot stress in the steel specimen is shown in Fig. 4. The point corresponding to a modulus of elasticity of zero represents results from the analysis of the specimen without an overlay. As the results show, the relationship between axial stiffness of the CFRP patch and HSS was parabolic in nature, indicating that there is a significant advantage associated with using an overlay, even if the modulus of elasticity of the composite material is relatively low. As Fig. 4 shows, HSS dropped by 58% with the introduction of an overlay with a very low modulus (26,600 MPa, 3,860 ksi) when compared to the unreinforced case. Increasing the modulus of elasticity of the

CFRP by a factor of five, from 26,000 MPa (3,860 ksi) to 138,000 MPa (20,000 ksi), led to a reduction in HSS by a factor of approximately three. These data show that increasing the modulus of elasticity of the CFRP material exhibits diminishing returns, which is important to consider when determining optimal configuration of the overlay. If infinite fatigue or propagation life can be achieved with a relatively inexpensive overlay, there is no economic incentive for using stiffer, and often much more expensive, fibers.

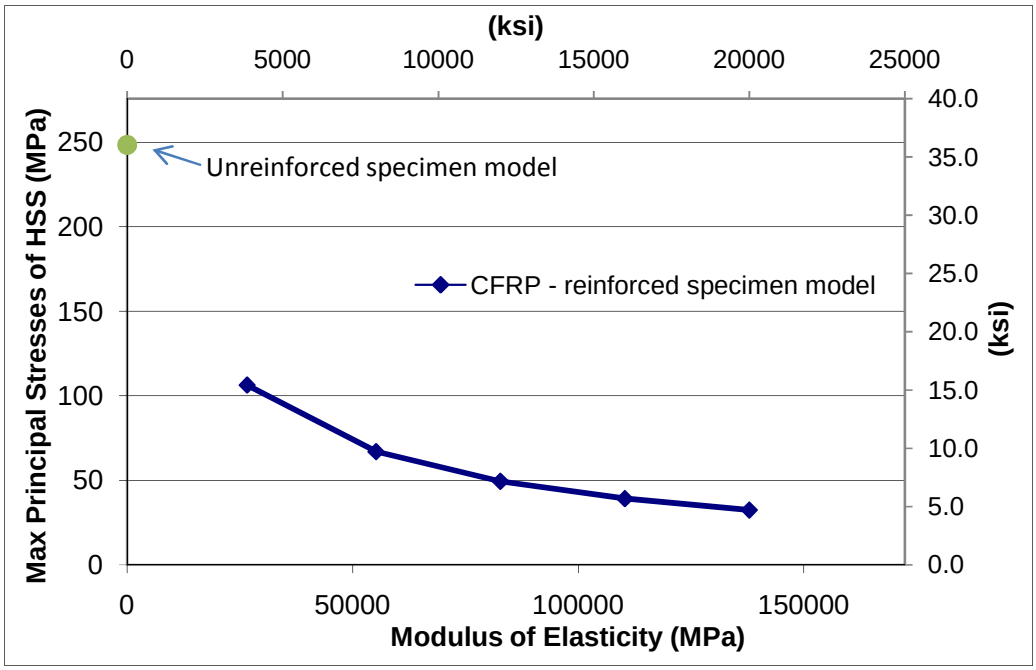

Figure 4 : Effect of the stiffness of the CFRP overlays on maximum principal Hot Spot Stresses in the steel specimen

Effect of the Thickness of the CFRP Overlay

The effect of the CFRP overlay thickness on HSS was evaluated using four different FE models. In these models all parameters were kept constant while the thickness of the CFRP overlay on one side was varied using values of 1.6, 3.2, 6.4, and 12.7 mm (0.063, 0.125, 0.250, and 0.500 in.). For all models discussed in this section, the modulus of elasticity of the overlay

was maintained at 83.0 GPa (12,000 ksi), the length of the CFRP overlay was kept as 457 mm (18.0 in.), and the thickness of the interface resin layer was held at 0.60 mm (0.025 in.). Results are presented in Fig. 5. The relationship between the CFRP overlay thickness and the maximum principal HSS was found to be inversely proportional. Similar to the behavior found when the CFRP modulus of elasticity was varied, increasing the thickness of the overlay exhibited diminishing returns, with the largest change in HSS observed between the unreinforced case and the case in which a 1.6 mm (0.06 in) thick overlay was utilized.

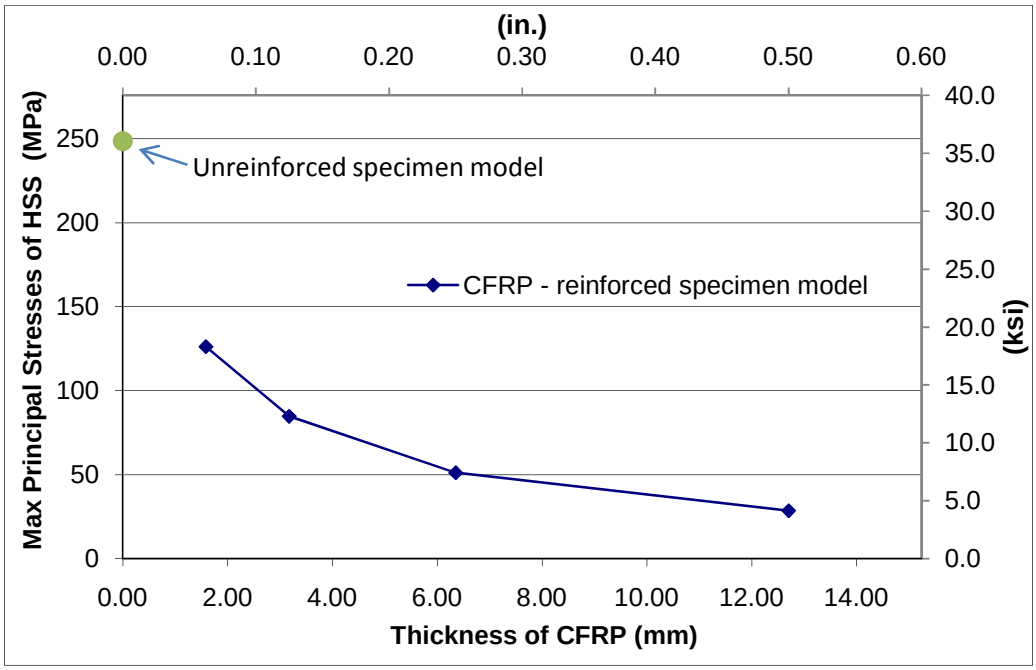

Figure 5 : Effect of the CFRP overlay thickness on maximum principal Hot Spot Stresses in the steel specimen

Effect of the Length of the CFRP Overlay

Six different configurations were defined to investigate the effect of the length of the CFRP overlay on the HSS along the critical path in the steel substrate. This effect was evaluated in terms of the total length of the CFRP overlay, with the overlay centered with respect to the

center of the hole of the steel specimen. A total of six models were developed, with overlay lengths varied from 152 mm (6.00 in.) to 457 mm (18.0 in.), which is a dimensional range equivalent to 24-72 hole diameters). For all models, the modulus of elasticity of the overlay was held at 83.0 GPa (12,000 ksi), the thickness of the CFRP overlay was maintained as 6.4 mm (0.25 in.), and the thickness of the interface layer was kept as 0.60 mm (0.025 in.). The results, presented in Fig. 6, show that there was a very small reduction in HSS in the steel substrate when the CFRP overlay length was changed from 152 mm (6.00 in.) to 203 mm (8.00 in.). For overlay lengths greater than 203 mm (8.00 in.) the effect of the overlay length on maximum principal HSS was found to be negligible.

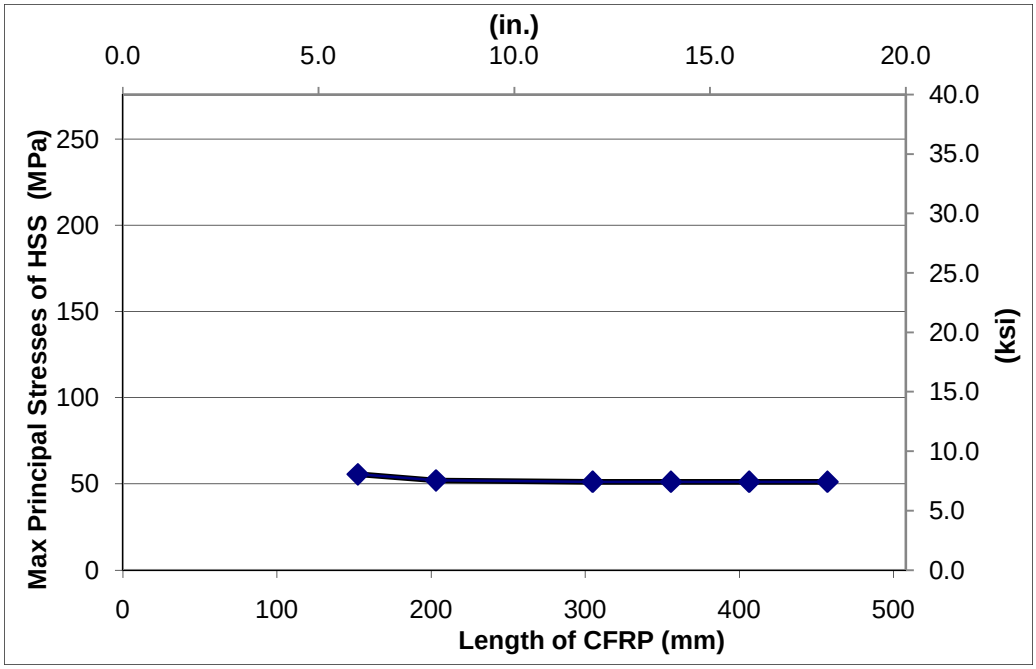

Figure 6 : Effect of the CFRP overlay length on maximum principal Hot Spot Stresses in the steel specimen

Effect of Thickness of Bond Layer

One of the parameters often neglected in FE simulations of retrofit measures with composite overlays is the flexibility inherent to the adhesive resin used to bond the overlay to the metal substrate. To achieve adequate bond, a resin with demonstrated acceptable adherence to steel must be employed. In most analyses found in the literature (Sabelkin et al. 2006; Liu, Xiao et al. 2009; Mall et al. 2009), it was assumed that the thickness of such a layer was very small, and that there was perfect bond between the composite and the substrate. Explicit modeling of this layer provides an indication of the average shear demand on the resin and the tensile demand on the resin-steel interface, which can be used to gage the potential for debonding. Because the shear and tensile demands on the resin are affected by the thickness of the resin layer, this is an important parameter to consider in terms of fatigue and fatigue crack propagation life.

A total of five different models were defined to investigate the effect of the thickness of the interface bond layer between the CFRP overlay and the steel substrate, with the interface layer thickness ranging from 0.60 mm (0.02 in.) to 5.0 mm (0.20 in.). For all models discussed in this section, the modulus of elasticity of the overlay was maintained as 82.7 GPa (12,000 ksi), the thickness of the CFRP overlay was kept as 6.4 mm (0.25 in.), the length of the CFRP overlay was held at 457 mm (18 in.), and the modulus of elasticity of the bond layer maintained as 2.1 GPa (300 ksi). The analyses results presented in Fig. 7 indicate that the maximum principal HSS was not affected by the thickness of the resin layer, suggesting that an increase in the thickness of the resin layer has a negligible effect on the effectiveness of the retrofit measure.

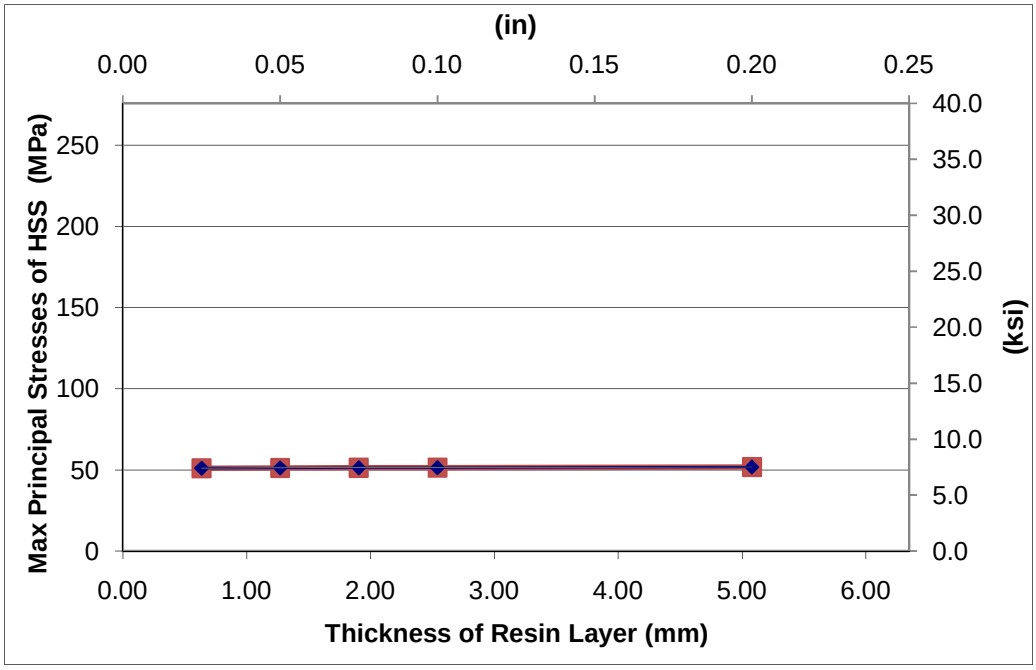

Figure 7 : Effect of the resin bond layer thickness on maximum principal Hot Spot Stresses in the steel specimen

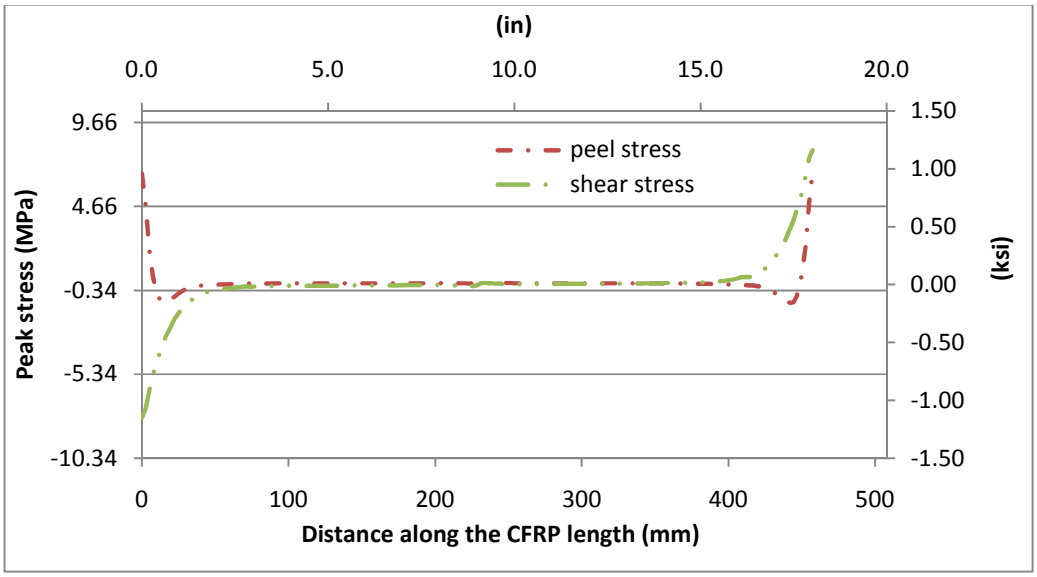

Figure 8 : Peak stresses along the CFRP overlay on resin layer end of hole

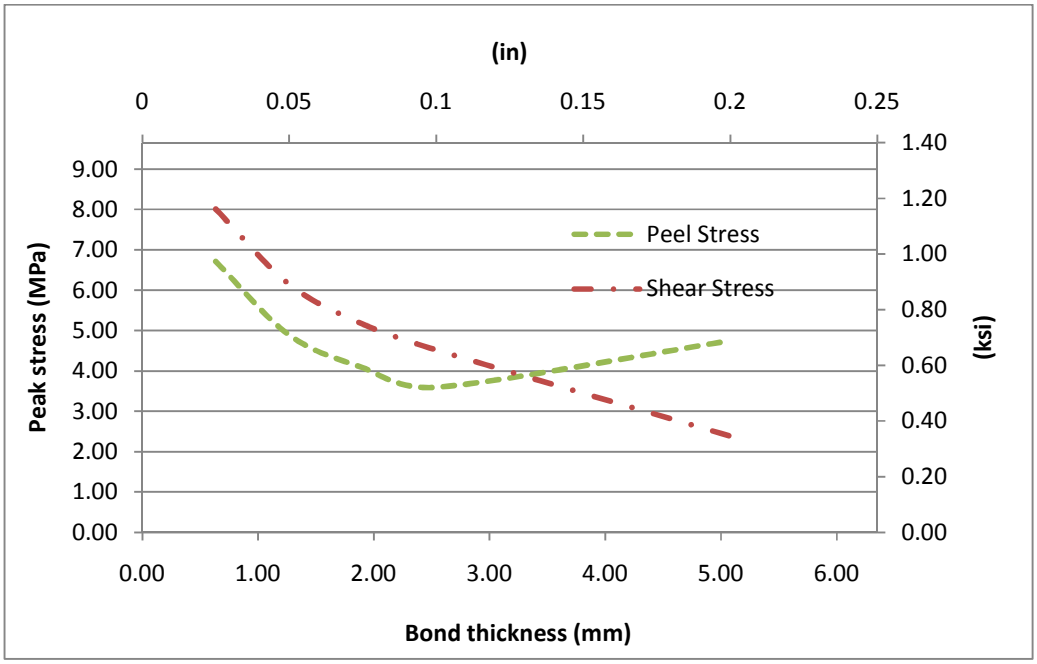

Figure 9 : Peak stresses demand on the CFRP layer as a function of resin layer thickness

Although the FE analyses showed that the thickness of the resin layer had a negligible effect on the HSS, another important design consideration is the effect of the thickness of the resin layer on the stress demand at the resin layer itself. This is important because maintaining bond between the composite and the steel is critical to the successful performance of the retrofit scheme, and higher stress demands increase the probability of fatigue failure at the interface. Fig. 8 shows the stress demand along the resin layer for a model with a layer thickness of 0.60 mm (0.02 in.). As Fig. 8 presents, the shear and peel stress (out of plane stress) demands are relatively low along most of the interface. Stress demands are greatest at both ends of the interface, and this is the location considered to be the most susceptible to fatigue failure.

Fig. 9 presents the variation of peak shear and peel stresses as a function of the thickness of the resin layer. The results show that increasing the interface layer thickness from 0.60 mm

(0.02 in.) to 5.0 mm (0.20 in.) caused a reduction in peak shear demand by approximately 66%. Fig. 9 also presents that the same increase in the thickness of the interface layer led to a reduction in peak peel stresses by approximately 40%. The trend observed for the peel stress was different from that observed for the shear stress in that the lowest peel stress demand was observed when an interface thickness of 2.5 mm (0.10 in.) was used, and any further increases in the thickness of the interface layer led to an increase in the peel stress. Fig. 7,8, and 9 show that although the thickness of the interface layer may not be relevant to fatigue crack propagation life due to negligible effect on the stress range, it is a very important parameter in terms of the bond performance of the interface layer under cyclic loading.

Results from the suite of FE analyses have shown that that the effect of the thickness of the interface resin layer and the length of the CFRP overlay on maximum principal HSS were much less significant than the effects of the thickness of the overlay and the modulus of elasticity of the CFRP, with the modulus of elasticity of the CFRP being the most significant of all four parameters.

Ratio of Overlay Axial Stiffness to Steel Axial Stiffness

As discussed in Section 1, one of the design parameters referenced in the literature for proportioning FRP patches is the ratio of axial stiffness of the composite patch to the axial stiffness of the underlying plate (Eq. 1). As Eq. 1 shows, this ratio may be modified by changing the modulus of elasticity of the FRP, the thickness of the FRP, or both. The results referenced in Sections 2.1 and 2.2 were used to derive two curves showing the effect of the stiffness ratio *SF* on the maximum principal HSS in the steel substrate. For each curve, one of the two parameters (modulus of elasticity of the FRP and thickness of the overlay) was varied while maintaining the

other constant. In all models discussed in this section, the length of the overlay was 457 mm (18.0 in.) and the thickness of the interface layer was 0.60 mm (0.025 in.). The results, presented in Fig. 10, show that changing the stiffness ratio *SF* by changing the modulus of elasticity of the CFRP had a more significant effect on the HSS than changing the *SF* ratio by altering overlay thickness. There was a common trend, in that sequential increments in the thickness of the overlay and the modulus of elasticity of the CFRP resulted in smaller reductions on the HSS. These results suggest that in terms of improving fatigue initiation life and fatigue crack propagation life, the configuration of the overlay is not as important as ensuring that the overlay remains bonded to the steel.

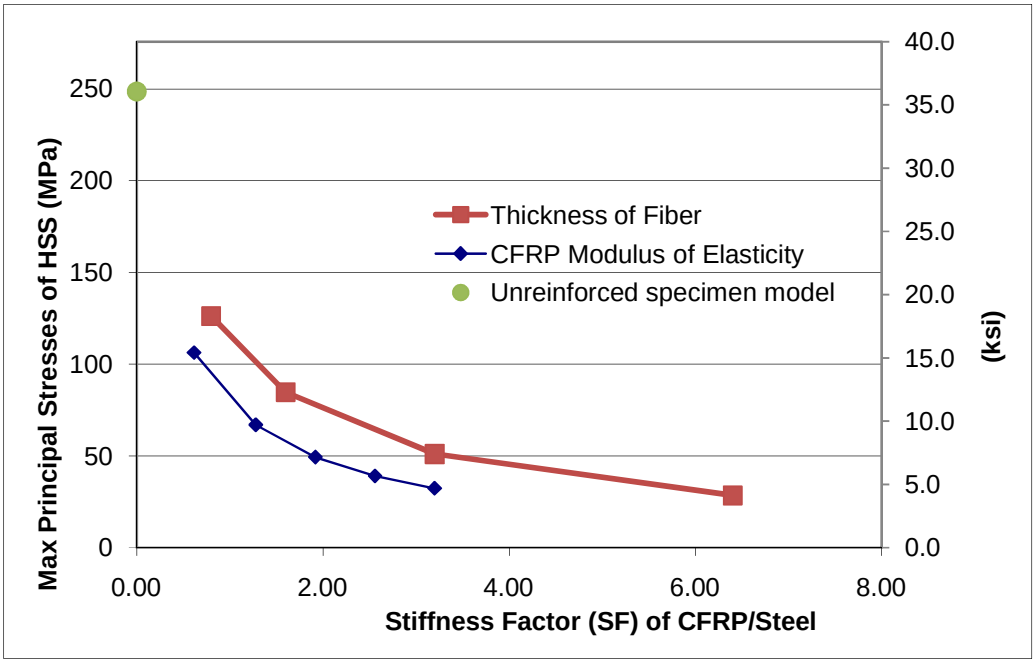

Figure 10 : Comparison the stiffness factors for the simulation results

Experimental Program

The goal of the experimental program was to evaluate the fatigue crack propagation lives of steel specimens with pre-existing fatigue cracks repaired using CFRP overlays under cyclic

loading. The CFRP overlay dimensions were selected to be 457 x 63 x 6.4 mm (18.0 x 2.50 x 0.25 in.), with composite overlays attached to both sides of the specimen. The thickness of the bond layer was selected 0.60 mm (0.025 in.).

Measured material properties are presented in Table 1. Coupon tests (ASTM 2000) from single-layered specimens showed that the modulus of elasticity of the CFRP was approximately 83.0 GPa (12,000 ksi). Liu et al. (2009) observed in their experiments that successive layers of CFRP in a repair patch experienced diminishing strain demands. For example, their measurements showed that the third layer of a composite overlay experienced 17 % of the strain of the first layer. Because measurements by Liu et al. (2009) showed that after the second layer the strain demand quickly dropped, the modulus of elasticity of the composite used for the computer simulations was selected to be between measured values for one and three layers.

The modulus of elasticity of the 9412 Hysol resin was also measured using coupon tests (Table 1) performed as prescribed by (ASTM 2000). The measured modulus of elasticity of the Hysol resin was 2.1 GPa (300 ksi).

Table 1 : Measured material properties

Continuous CFRP

No. of Layers in Coupon	No. of Coupons	Avg. Modulus of Elasticity *GPa (ksi)*	Standard Deviation *GPa (ksi)*
1	3	85.8 (12,440)	10.0 (1,450)
3	4	75.3 (10,930)	10.9 (1,580)
5	3	61.7 (8,940)	0.3 (42.0)

9412 Hysol Resin

Coupon Thickness *mm (in.)*	No. of Coupons	Avg. Modulus of Elasticity *GPa (ksi)*	Standard Deviation *GPa (ksi)*

6.4 (0.25)	6	2.1 (303)	0.2 (25)

Chopped-CFRP Composite

Coupon Thickness *mm (in.)*	No. of Coupons	Avg. Modulus of Elasticity *GPa (ksi)*	Standard Deviation *GPa (ksi)*
4.8 (0.19)	7	14.1 (2,052)	6 (866)

Table 2 summarizes the test matrix for the experimental program. Two unreinforced control specimens were tested with nominal stress ranges of 166 MPa (24.0 ksi) and 221 MPa (32.0 ksi). Two specimens with different types of composite overlays were tested at a stress range of 166 MPa (24.0 ksi). A third specimen, repaired with CFRP overlays was tested at a higher stress range of 221 MPa (32 ksi).

Table 2 : Specimen test matrix

Specimen Designation	**Overlay Type**	**Stress Range *MPa (ksi)***	**Number of Cycles**	**Final Crack Size mm (in)**
Control 1	None	221 (32)	18,000	Total Failure
Control 2	None	166 (24)	55,000	Total Failure
F 9	14-Layer CFRP	221 (32)	3,000,006	5.08 (0.20)
F 10	Chopped-CFRP	166 (24)	1,084,699	2.79 (0.11)
F 12	14-Layer CFRP	166 (24)	4,059,048	5.08 (0.20)

Specimen Dimensions

The specimens were fabricated using grade A36 steel and were 3.20 mm (0.125 in.) thick. The stress-strain relationship obtained for the steel is presented in Fig. 11. The measured yield strength of the steel was 303 MPa (44.0 ksi), and the tensile strength was 460 MPa (66.7 ksi).

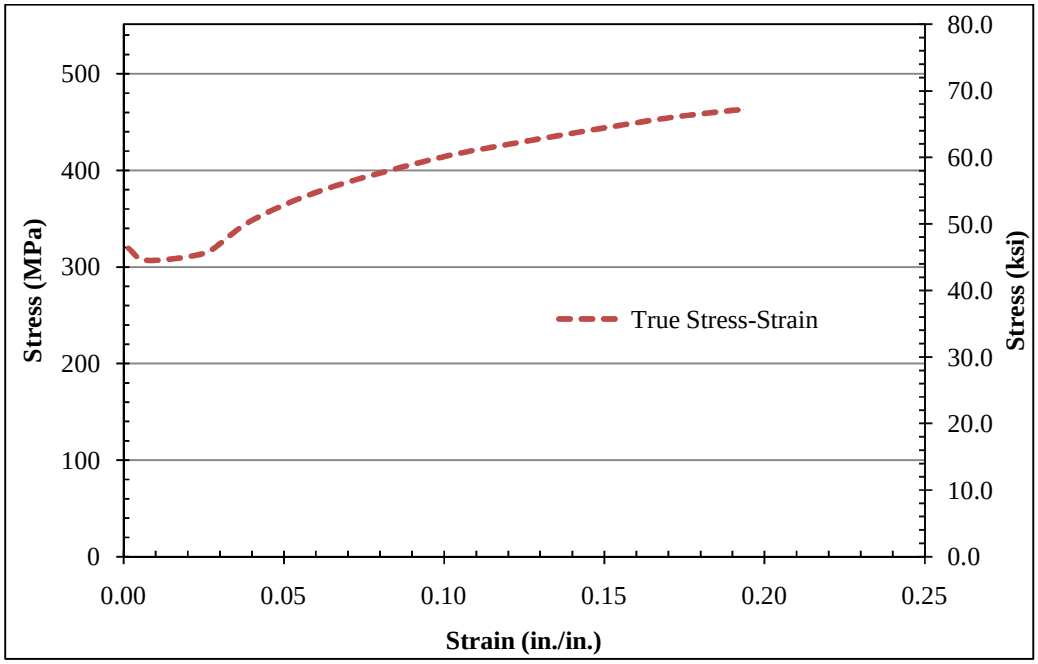

Figure 11 : Stress strain curve for the specimen

Specimen dimensions are shown in Fig. 1. Each specimen had a drilled and reamed hole at the center of the specimen with a diameter of 3.20 mm (0.125 in.). Both sides of the hole had pre-existing fatigue cracks with a length of approximately 2.5 mm (0.1 in.), created by loading the specimens under repeated cycles at a constant stress range.

Surface preparation

Maintaining bond under cyclic loading is critical to the successful performance of the repair method discussed in this paper. To develop adequate bond, the steel surface was prepared by a process of abrading and cleaning. Abrading consisted of roughening of the surface with a hand grinder to achieve a surface roughness of approximately 0.80 mm (0.031 in.). After abrading, cleaning of the surface was performed using acetone and methanol.

Fabrication of the Multi-Layered CFRP Overlays

The multi-layered CFRP overlays were pre-fabricated and subsequently attached to the steel specimens. Each CFRP overlay had 14 layers of bi-directional pre-impregnated carbon fiber ply for a total thickness of 6.4 mm (0.25 in.). Although previous experimental results (Liu et al. 2009) showed that the strain demand in the CFRP plies after the third layer were small compared with those in the first and second layers, the overlay was fabricated with a total of 14 layers to facilitate removal for inspection and reuse.

Each layer was fabricated using a single pre-impregnated carbon fiber ply, with a sheet of Scotch-Weld Epoxy adhesive (1838 B/A Green) added every fourth layer of carbon fiber ply, to ensure that there was a sufficient amount of resin to prevent voids from occurring between resin layers during the curing process. The thickness of the overlay was controlled during the fabrication process by using a mold consisting of aluminum plates placed between bolted steel plates, as shown in Fig. 12. The fabrication process is described in the following. First, the pre-impregnated CFRP plies were cut to dimensions of approximately 457 x 152 mm (18.0 x 6.00 in.), which was double the size of the overlays. The FRP sheets were placed on the bottom steel plate of the mold, and were added one layer at a time. Every fourth layer, a single sheet of Scotch-Weld Epoxy adhesive (1838 B/A Green) resin with the same dimensions was added.

The CFRP was surrounded by an aluminum spacer with a thickness of 6.4 mm (0.25 in.). Due to voids in the interfaces between layers of CFRP plies, the total thickness of the overlay was greater than the target 6.4 mm (0.25 in.) after all 14 layers of CFRP plies were placed in the mold. The top steel plate of the mold was then placed on top of the CFRP stack, and pressure was applied by tightening the bolts around the perimeter of the mold. At this point, the overlay was placed in the oven for curing. The curing oven was preheated to a temperature of 175 C

(347 *F)*. The CFRP overlays were cured inside the metal mold for three hours, and subsequently allowed to cool to room temperature for 48 hours. After the curing process was completed, the CFRP overlays were taken out of the metal molds and cut to final dimensions of 457 x 64.0 mm (18.0 x 2.50 in.) using a diamond saw. Sand paper (grade 400) was used to smooth the edges of the CFRP. A hole was drilled in the middle of the CFRP overlays with a diameter of 3.18 mm (0.125 in.) to facilitate alignment with the steel specimen.

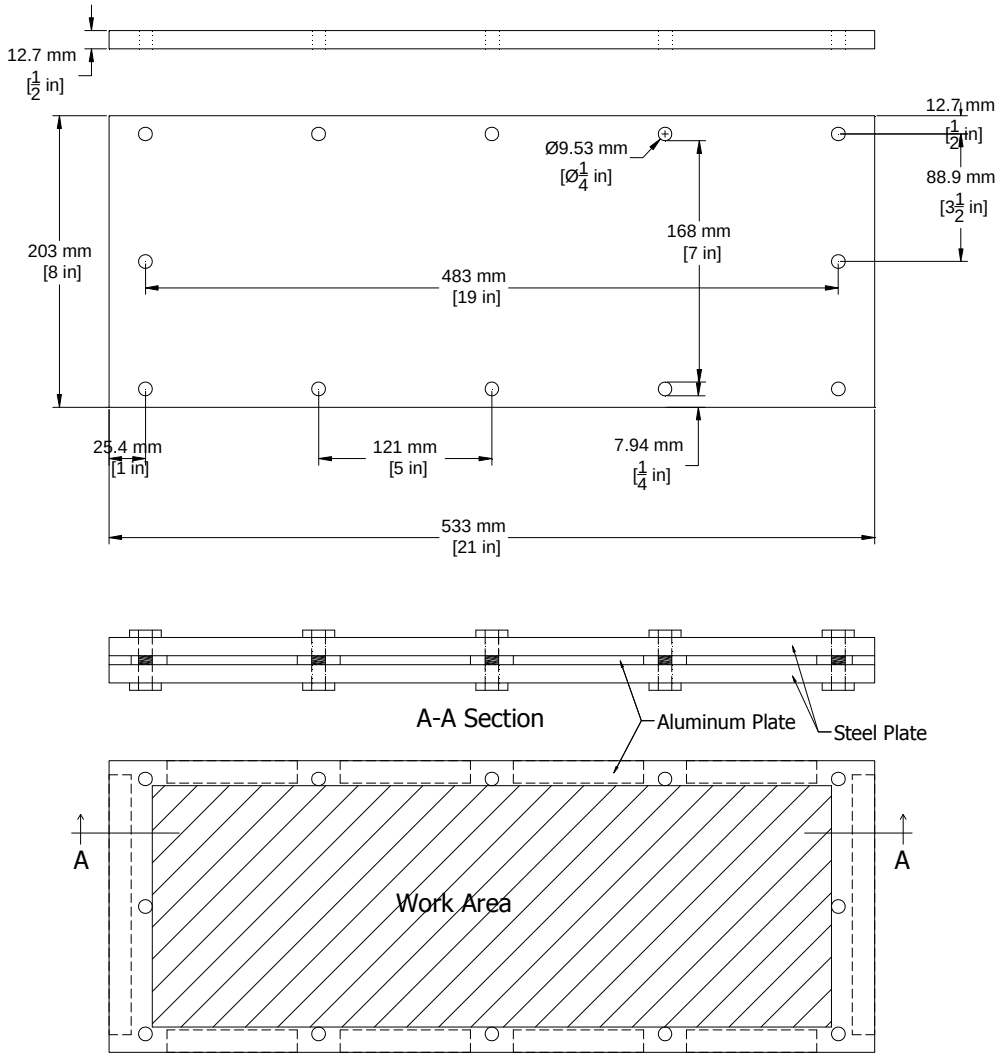

Figure 12 : Steel plates for making FRP plate

The CFRP overlays were attached to the steel specimen using Hysol® 9412 epoxy resin, which has a nominal shear strength of 28 MPa (4 ksi) (Hysol®). The thickness of the Hysol® layer was 0.60 mm (0.024 in.), maintained during fabrication by using six spacers evenly distributed throughout the interface. Drafting tape surrounding the steel plate was used to prevent leaking of the Hysol® resin by creating a resin pool. A bolt was used to align the steel plate and the two CFRP overlays at the center hole. Hysol® resin was poured inside the taped-off area, and pressure was applied using grips to maintain the thickness of the interface layer at 0.60 mm (0.024 in.). After two days of curing the interface bond layer, final preparation was performed by cleaning the specimen from remnant resin using a chisel and a heat gun.

Fabrication of CFRP Chopped-Fiber Overlays

Use of chopped-CFRP overlays was also investigated to evaluate the performance of this composite material in terms of fatigue-crack propagation life; this was an attractive alternative to consider, due to simpler composite fabrication. The chopped fiber overlays were fabricated using an external mixing spray machine (a non-atomized resin lel chopper system commercialized by BINKS). The spray machine used a vinyl-ester resin with Norox MEKP-925 catalyst and graphite fiber yarn. The surface preparation performed was the same as that described in Section 3.2. After surface preparation and subsequent cleaning, the fiber-resin mix was sprayed on steel substrate in layers approximately 3.2 mm (0.13 in) thick, and was compacted using a hand tool until the average thickness of the composite overlay was 6.4 mm (0.25 in). The specimen was cured at room temperature for two days, after which the remnant resin was cleaned from the specimen.

Test procedure

A cyclic tensile load was applied at the ends of the specimen using an MTS closed-loop servo-controlled loading system. The applied load was determined on the basis of the nominal stress demand at the net section of the steel specimen, calculated using the actual (measured) net cross sectional area without any adjustments for stress concentration in the area surrounding the hole. These values, although not representative of the peak stress demand, were adopted to simplify the comparison between various specimens. The ratio of minimum to maximum stress was maintained constant at R=0.1. The rate of fatigue-crack propagation was evaluated at two different stress ranges, 221 MPa (32.0 ksi) and 166 MPa (24.0 ksi). A maximum tension load of 19.4 kN (4.36 kips) corresponded to a stress range at the middle section of 221 MPa (32.0 ksi). Upon loading, crack growth was monitored periodically. Every million cycles, the CFRP overlays were removed to measure the crack size and subsequently reattached for additional loading cycles. The reattachment procedures were the same as described in Section 3.3.

Experimental Results

The propagation life of the steel specimens used in this study was calculated for different stress range demands based on established theoretical expressions, as presented in Fig. 13. The relationship between crack length and number of cycles was calculated using the following expression (Barsom and Rolfe, 1999):

$$\frac{da}{dN} = A(\Delta K)^m \qquad (2)$$

where a is crack length, N is the number of cycles, A and m are material constants, and ΔK is a stress intensity factor range. Material constants of A=10E-10 and m=3 were adopted, which correspond to values for ferrite-pearlite steel (Barsom and Rolfe, 1999). The stress

intensity factor depends on the ratio of crack length to plate width (*a*/*b*) and the ratio of crack length to hole radius (*a*/*r*) (Barsom and Rolfe, 1999). Stress intensity factors for various *a*/*b* and *a*/*r* ratios listed by Barsom and Rolfe (1999) were used.

As shown in Fig. 13, the parameters in the expression provided a close correlation between the fatigue-crack propagation life of unrepaired specimens and the theoretical propagation life for the corresponding stress range.

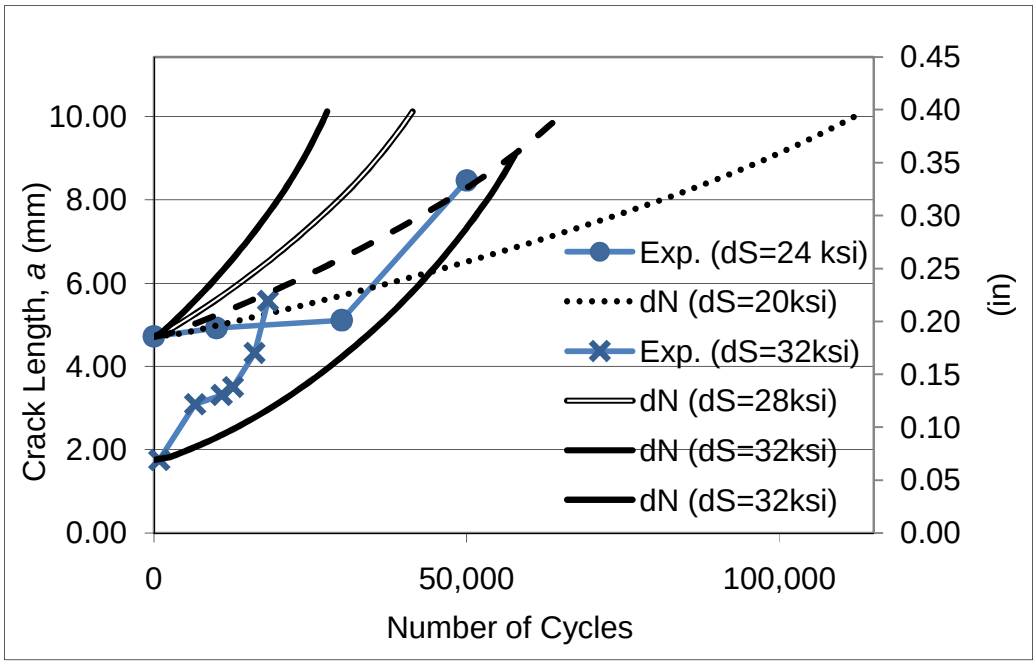

Figure 13 : Comparison between theoretical and experimental values for the fatigue-crack propagation life of unreinforced specimens

As indicated in Section 3, the two nominal stress ranges that the specimens were tested at were 221 MPa (32.0 ksi) and 166 MPa (24.0 ksi). These values were computed by dividing the applied force by the cross sectional area at the nt section of the specimen, which was approximately 90.3 mm^2 (0.140 in^2). A comparison between observed fatigue-crack

propagation rate in specimens with CFRP overlays and the calculated fatigue-crack propagation rate in unreinforced specimens with low stress demands is presented in Fig. 14.

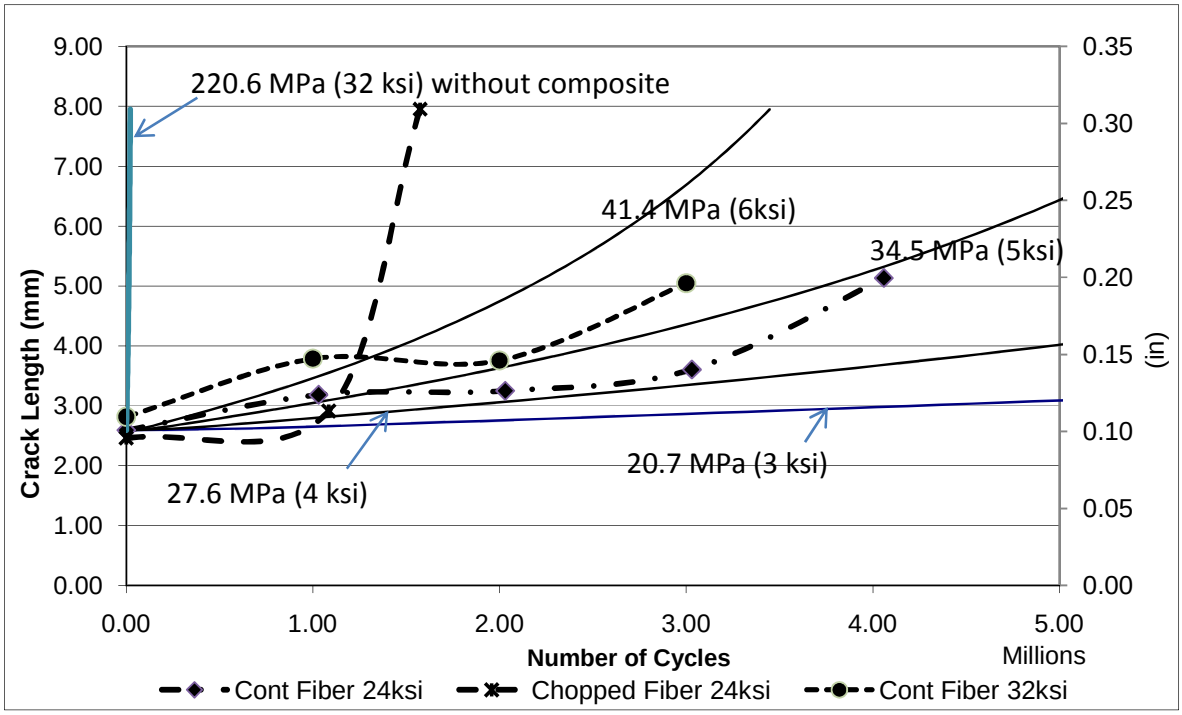

Figure 14 : Comparison of crack propagation between specimens with CFRP overlays and theoretical values for specimens without overlays

As shown in Fig. 14, the crack propagation rate of a specimen repaired with continuous CFRP fibers subjected to a stress range of 166 MPa (24.0 ksi) was similar to that of an unrepaired specimen subjected to a stress range of 35 MPa (5 ksi) theoretical values. These results indicate that the presence of the overlay resulted in a reduction of approximately 80% in the stress range. The test of the specimen repaired with multi-layered CFRP overlay subjected to a stress range of 166 MPa (24 ksi) was stopped after 4 million cycles, after the crack growth started to become noticeable. Had the fatigue crack in this specimen continued to propagate at the theoretical rate for an unreinforced specimen under a stress range of 35 MPa (5 ksi), it would

have reached a crack length of 7.6 mm (0.3 in.) at approximately 6 million cycles. A similarly loaded unrepaired steel specimen reached a crack length of 7.6 mm (0.3 in.) at only 50,000 cycles (Fig. 13).

The fatigue crack propagation life of the continuous-fiber CFRP repaired specimen subjected to a stress range of 221 MPa (32 ksi) was greater than 3 million cycles. At this point the test was stopped after noticing measurable crack growth. The comparison between unrepaired and continuous-fiber CFRP repaired cases shows that the increase in fatigue-crack propagation life provided by the continuous-fiber CFRP repair was more than 50 times with respect to an unreinforced specimen. The repaired specimen subjected to a stress range of 221 MPa (32 ksi) had a nominal maximum stress of 235 MPa (34.0 ksi), which was close to the measured yield stress of 303 MPa (44.0 ksi) for the steel. The results show that the behavior of the continuous-fiber CFRP repaired specimen was similar to that of an unrepaired specimen subjected to a nominal stress range between 35 (5 ksi) and 41 MPa (6 ksi), which indicates that the CFRP repair was very effective at that high stress range as well.

The experimental fatigue-crack propagation curves shown in Fig. 14 also indicate that rate of crack growth in repaired specimens had a greater tendency to increase with crack size than the theoretical relationship for unreinforced specimens (Eq. 2). This could be an indication that as the fatigue crack grows, the bond between the composite and the steel in the area surrounding the crack is reduced, making the repair less effective. It is hypothesized that this detrimental effect could be lessened by drilling a hole at the tip of the crack, to remove the sharp crack tip and the process zone. The combination of the stress reduction due to the alternate load path provided by the composite and the repair of the tip of the crack may be sufficient to drive

the stress demand below the fatigue-crack-propagation threshold (Barsom and Rolfe, 1999). This is a combination of techniques that warrants future study.

Average crack propagation rates are presented in Table 3. The experimental curves were divided into two regions. During early fatigue crack growth the propagation rate was nearly constant. Average rates of crack growth for the nearly constant region are presented in the third row of Table 3. After a significant amount of crack growth, the crack propagation rate increased as the specimens approached failure and, in the case of specimens with overlays, the bond between the overlay and the steel degraded. The values in Table 3 show that for specimens with a stress range of 166 MPa (24.0 ksi) the effect of the overlays was to decrease the crack growth rate by a factor of approximately 45, and the reduction in the rate of crack growth was similar for both types of composite overlays. For the specimen subjected to a stress range of 221 MPa (32 ksi), the bonding of the overlays resulted in a reduction in the crack growth rate by a factor of approximately 300.

Table 3 : Average crack propagation growth rates

$\Delta\sigma$ *MPa (ksi)*	166 (24)	221 (32)	166 (24)	166 (24)	221 (32)
Type of Overlay	None	None	Multi-Layered	Chopped Fiber	Multi-Layered
Average Crack Propagation Rate, Stable growth, μ m/cycle (μ in./cycle)	0.0147 (0.58)	0.1575 (6.19)	0.00025 (0.01)	0.0005 (0.02)	0.0005 (0.02)

Conclusions

The results of study of using carbon fiber reinforced polymer (CFRP) to repair fatigue crack in steel plates resulted in the following conclusions:

- Experimentally observed reductions in stress range demand associated with the bonding of overlays were consistent with those observed in Finite Element simulations.
- Experimental results showed that bonding of pre-fabricated multi-layered CFRP overlays extended the fatigue-crack propagation lives of the steel specimens by more than 50 times. The observed increase in fatigue-crack propagation life was significantly higher than values ranging between 4.7 and 7.9 reported in previous studies on aluminum plates, steel plates, and steel beams. The main difference between the overlays used in this study and those used in other studies found in the literature is that the stiffness ratio *SF* was significantly higher.
- The computer simulations showed that for the repair of steel plates with bonded CFRP overlays, the parameters that have the most significant effect on fatigue-crack propagation life were the modulus of elasticity of the CFRP and the thickness of the overlay.
- Maintaining adequate bonding between the CFRP overlay and the steel is critical. Significantly better performance was obtained by using a high-quality bonding resin over direct spraying of the composite on the steel.
- Although the increase in fatigue-crack propagation life was less for the sprayed overlay, the increase was on the order 30 times the propagation life of an unreinforced composite.

Research has shown that use of CFRP as a repair technique in cracked steel members can be a highly effective means of reducing stress demand and greatly prolonging the propagation

life of the steel member. This method works well with steel members because of the higher stiffness ratios of the CFRP overlays.

References:

AASHTO, L. 2004. Bridge Design Specifications (2004). *American Association of State Highway and Transportation Officials*.

Albrecht, P., and A. Lenwari. 2007. Fatigue-proofing cover plates. *Journal of Bridge Engineering* 12 (3):275-283.

ASTM, D. 2000. 3039/D 3039M,". *Standard Test Method for Tensile Properties of Polymer Matrix Composite Materials*.

Barsom, JM, and ST Rolfe. 1999. *Fracture and fatigue control in structures: applications of fracture mechanics*. Vol. 3rd: ASTM International.

Cartwright, DJ, and DP Rooke. 1976. The compounding method applied to cracks in stiffened sheets. *Engineering Fracture Mechanics* 8:567-563.

Kaan, B, R Barrett, C Bennett, A Matamoros, and S Rolfe. 2008. Fatigue Enhancement of Welded Coverplates Using Carbon Fiber Composites.

Lee, W. Y., and J. J. Lee. 2004. Successive 3D FE analysis technique for characterization of fatigue crack growth behavior in composite-repaired aluminum plate. *Composite Structures* 66 (1-4):513-520.

Liu, H. B., R. Al-Mahaidi, and X. L. Zhao. 2009. Experimental study of fatigue crack growth behaviour in adhesively reinforced steel structures. *Composite Structures* 90 (1):12-20.

Liu, H. B., Z. G. Xiao, X. L. Zhao, and R. Al-Mahaidi. 2009. Prediction of fatigue life for CFRP-strengthened steel plates. *Thin-Walled Structures* 47 (10):1069-1077.

Mall, S, and DS Conley. 2009. Modeling and validation of composite patch repair to cracked thick and thin metallic panels. *Composites Part A: Applied Science and Manufacturing* 40 (9):1331-1339.

Mall, S., and D. S. Conley. 2009. Modeling and validation of composite patch repair to cracked thick and thin metallic panels. *Composites Part a-Applied Science and Manufacturing* 40 (9):1331-1339.

Marquis, G, and A Kaehoenen. 1995. Fatigue testing and analysis using the hot spot method.

Naboulsi, S, and S Mall. 1996. Modeling of a cracked metallic structure with bonded composite patch using the three layer technique. *Composite Structures* 35 (3):295-308.

Nakamura, H., W. Jiang, H. Suzuki, K. Maeda, and T. Irube. 2009. Experimental study on repair of fatigue cracks at welded web gusset joint using CFRP strips. *Thin-Walled Structures* 47 (10):1059-1068.

Petri, B. 2008. Finite element analysis of steel welded coverplate including composite doublers, University of Kansas.

Sabelkin, V, S Mall, and JB Avram. 2006. Fatigue crack growth analysis of stiffened cracked panel repaired with bonded composite patch. *Engineering Fracture Mechanics* 73 (11):1553-1567.

Sabelkin, V., S. Mall, M. A. Hansen, R. M. Vandawaker, and M. Derris. 2007. Investigation into cracked aluminum plate repaired with bonded composite patch. *Composite Structures* 79 (1):55-66.
Schubbe, J. J., and S. Mall. 1999. Investigation of a cracked thick aluminum panel repaired with a bonded composite patch. *Engineering Fracture Mechanics* 63 (3):305-323.
Schubbe, JJ, and S Mall. 1999. Modeling of cracked thick metallic structure with bonded composite patch repair using three-layer technique. *Composite Structures* 45 (3):185-193.
Tavakkolizadeh, M, and H Saadatmanesh. 2003. Fatigue strength of steel girders strengthened with carbon fiber reinforced polymer patch. *Journal of Structural Engineering* 129 (2):186-196.
Umamaheswar, TVRS, and R Singh. 1999. Modelling of a patch repair to a thin cracked sheet. *Engineering Fracture Mechanics* 62 (2-3):267-289.
Vilhauer, B. 2007. Fatigue behavior of welded connections enhanced with UIT and bolting, University of Kansas.
ABAQUS, Version 6.8-2, Simulia, 2009, http://www.simulia.com.
Barsom, J.M., and Rolfe, S.T. (1999). "Fatigue and fracture behavior of welded components." *Fracture and Fatigue Control in Structures*, 3rd ed., (10), American Society for Testing and Materials, West Conshohocken, PA, 35-53.
Roy, M., Lang, C., & May, I. (2009). Modelling composite repairs to cracked metal structures. Proceedings of the Institution of Civil Engineers. *Structures and Buildings*, 162(2), 107-113.
Hysol® 9412, Loctite 9412 Hysol Epoxy Adhesive, 2001, http://www.henkelna.com.

Acknowledgment

The authors are grateful for support from the Kansas Department of Transportation (KDOT) and the University of Kansas Transportation Research Institute (KU TRI). The authors would also like to appreciatively acknowledge support provided through Pooled Fund Study TPF-5(189), which includes the following participating State DOTs: Kansas, California, Iowa, Illinois, New Jersey, New York, Oregon, Pennsylvania, Tennessee Wisconsin, and Wyoming, as well as the Federal Highway Administration.